Electronic Supplementary Information

Helical aromatic imide based enantiomers with full-color circularly polarized luminescence

Meng Li,[a] Hai-Yan Lu,[b,*] Chao Zhang,[b] Lin Shi,[c] Zhiyong Tang,[c] and Chuan-Feng Chen[a,*]

[a]*Beijing National Laboratory for Molecular Sciences, CAS Key Laboratory of Molecular Recognition and Function, Institute of Chemistry, Chinese Academy of Sciences, Beijing 100190, China. E-mail: cchen@iccas.ac.cn*

[b]*University of Chinese Academy of Sciences, Beijing 100049, China. E-mail: haiyanlu@ucas.ac.cn*

[c]*Laboratory of Nanomaterials, National Center for Nanoscience and Technology, Beijing 100190, China.*

Contents

1. General information

All the reagents and solvents were commercially available and used without further purification. Reactions were carried out under inert and anhydrous conditions unless otherwise noted. ^{1}H, ^{13}C, ^{19}F NMR spectra were recorded on Bruker® Avance 300MHz, Brucker® Avance III 400 MHz, Brucker® AVIII 500 MHz NMR, and Brucker® AVIII 600 MHz NMR spectrometers in $CDCl_3$ solutions at 298 K. All the melting points were not calibrated and determined on YuHua X-5 digital melting point apparatus. High resolution mass spectra were obtained on the Thermo Fisher® Exactive high-resolution LC-MS spectrometer. The X-ray crystallographic data were collected by Rigaku® X-ray diffraction apparatus RAPID IP, MM007HF Saturn 724+, ST Saturn 724+. Optical resolutions were carried out on supercritical fluid chromatography (SFC) using the column (Chiralpak® IC, 4.6 cm × 150 mm) and the mobile phase of CO_2/MeOH/DCM (40:30:30, *v*/*v*/*v*). HPLC analysis were performed on Agilent 1260 Infinity. Analytical injections were performed on chiral stationary phase using the column (Chiralpak® IC, 5 μm, 4.6 mm × 250 mm) and the mobile phase of hexane and dichloromethane (60:40, *v*/*v*). The UV-vis spectra were recorded on PerkinElmer® UV/Vis/NIR spectrometer (Lambda 950), and the fluorescence spectra were recorded on HITACHI® F-7000 Fluorescence Spectrometer at room temperature. Absolute fluorescence quantum yield, measured by Hamamatsu Absolute PL Quantum Yield Spectrometer C11347. Fluorescence lifetimes were measured by Quantaurus Tau C11367–11. CD spectra were recorded on a JASCO J810 spectropolarimeter, and CPL spectra were performed with a JASCO CPL-200 spectrometer at room temperature. The optical rotation was determined by Rudolph Autopol VI Automatic polarimeter. The starting diene **2** was synthesized by reported method.[1]

2. Synthetic procedures and characterized data

Synthesized of racemic synthon

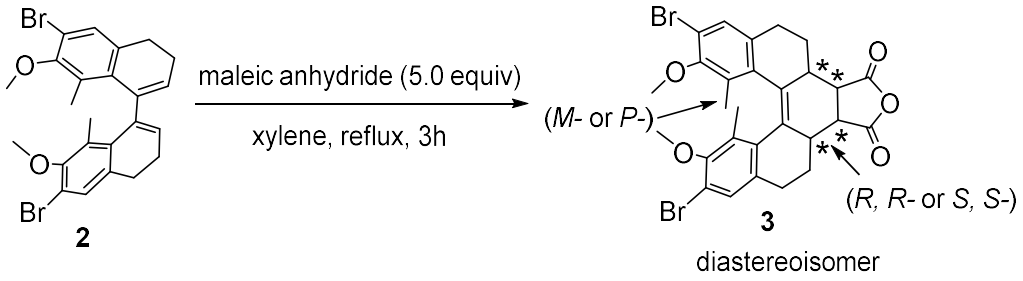

Diastereoisomers 3. To a solution of diene **2** (10.24 g, 20.32 mmol) in xylene (100 mL) was added maleic anhydride (9.8 g, 0.1 mol, 5.0 equiv) with vigorous stirring, followed by reflux for 3 h. After the reaction mixture was cooled to room temperature, the solvent was removed by rotatory evaporation to give crude product, which was further purified by recrystallization in acetic acid to give diastereoisomers **3** (10.9 g, 89%) as white powder. ^{1}H NMR (500 MHz, $CDCl_3$): δ 7.33 (d, J = 4.7 Hz, 2H), 3.51 (d, J = 12.2 Hz, 6H), 3.17 (t, J = 9.8 Hz, 1H), 3.02–2.98 (m, 1H), 2.93–2.83 (m, 2H), 2.81–2.74 (m, 2H), 2.70–2.60 (m, 1H), 2.63–2.60 (m, 1H), 2.51–2.37 (m, 2H), 1.66–1.60 (m, 1H), 1.24 (s, 3H), 1.15 (s, 3H). ^{13}C NMR (126 MHz, $CDCl_3$): δ 172.4, 171.3, 154.70, 154.65, 139.0, 138.7, 136.24, 136.17, 134.89, 134.88, 131.3, 129.8, 129.3, 116.3, 116.2, 59.84, 59.82, 45.5, 45.0, 40.3, 37.5, 30.8, 27.3, 26.7, 25.9, 14.8, 14.2. HRMS (APCI): *m/z* calcd for $C_{28}H_{27}Br_2O_5$ $[M + H]^+$ 603.0199, found 603.0220.

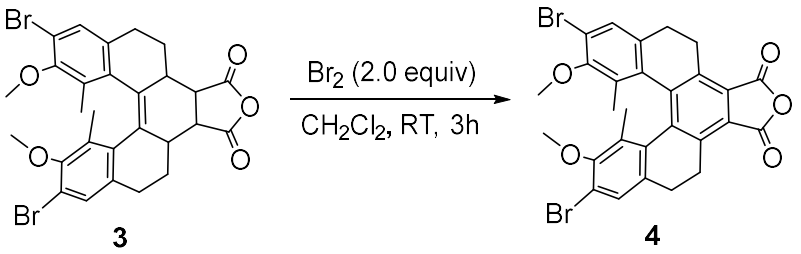

Compound 4. To a solution of **3** (30.1 g, 50 mmol) in CH_2Cl_2 (150 mL), bromine (16 g, 0.1 mol) in acetic acid (15 mL) was added slowly at room temperature. After the reaction mixture was stirred for another 3 hours, saturated aqueous Na_2SO_3 was added. The organic layer was concentrated in *vacuo* to give a crude product, which was further purified by recrystallization from ethyl acetate / petroleum ether to afford compound **4**

(16.8 g, 56%) as yellow solid. M. p.: > 300 °C. ^{1}H NMR (500 MHz, $CDCl_3$): δ 7.49 (s, 2H), 3.96 (ddd, *J* = 15.7, 3.8, 2.1 Hz, 2H), 3.55 (s, 6H), 2.95 (ddd, *J* = 14.5, 4.2, 2.3 Hz, 2H), 2.70–2.62 (m, 2H), 2.57–2.48 (m, 2H), 1.28 (s, 6H). ^{13}C NMR (126 MHz, $CDCl_3$): δ 163.0, 155.1, 141.0, 140.8, 137.6, 134.6, 131.1, 129.9, 124.7, 117.7, 59.9, 29.7, 24.3, 14.6. HRMS (APCI): *m/z* calcd for $C_{28}H_{23}Br_2O_5$ $[M + H]^+$ 598.9886, found 598.9898.

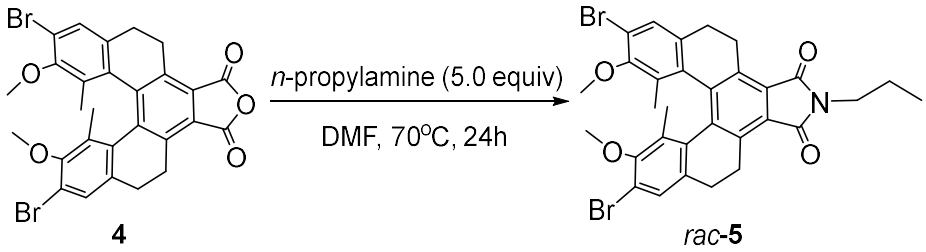

Compound *rac*-5. A mixture of **4** (12.0 g, 20 mmol) and *n*-propylamine (5.9 g, 0.1 mol) in DMF (100 mL) was stirred at 70 °C for 24 hours. After the reaction mixture was cooled to room temperature, it was poured into ethyl acetate (100 mL). The organic layer was washed with saturated brine (3×100 mL), dried over anhydrous $MgSO_4$, and then concentrated in *vacuo*. The residue was purified by flash column chromatography with ethyl acetate, dichloromethane and petroleum ether (0.2:1:3, *v*/*v*/*v*) as eluent to give the compound *rac*-**5** (10.5 g, 82%) as pale-yellow solid. R_f = 0.46. M. p.: 220-222 °C. ^{1}H NMR (300 MHz, $CDCl_3$): δ 7.46 (s, 2H), 4.10 (dt, *J* = 15.6, 3.0 Hz, 2H), 3.65 (dt, *J* = 7.4, 4.0 Hz, 2H), 3.54 (s, 6H), 2.90 (dt, *J* = 14.3, 3.1 Hz, 2H), 2.63 (td, *J* = 14.5, 3.7 Hz, 2H), 2.44 (td, *J* = 15.1, 3.9 Hz, 2H), 1.73 (h, *J* = 7.3 Hz, 2H), 1.28 (s, 6H), 0.98 (t, *J* = 7.4 Hz, 3H).^{13}C NMR (75 MHz, $CDCl_3$): δ 168.8, 154.9, 138.8, 138. 7, 137.9, 135.3, 131.0, 129.6, 125.4, 116.9, 59.8, 39.5, 29.5, 24.0, 22.0, 14.6, 11.4. HRMS (APCI): *m/z* calcd for $C_{31}H_{30}Br_2NO_4$ $[M + H]^+$ 640.0516, found 640.0507.

Optical resolution

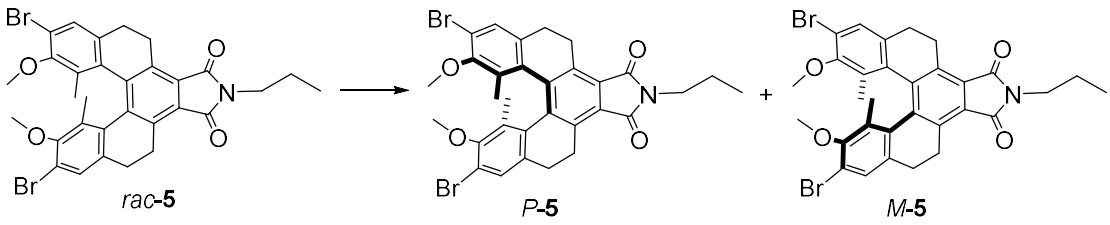

Efficiently semi-preparative optical resolution of *rac*-**5** was performed by

supercritical fluid chromatography (SFC), which provided the pair of enantiomers *P*-**5** and *M*-**5** (ee > 99%) in gram scale (for detail, see ***HPLC charts***).

General procedure for the synthesis of enantiomers 1a-e by suzuki-miyaura cross coupling reactions

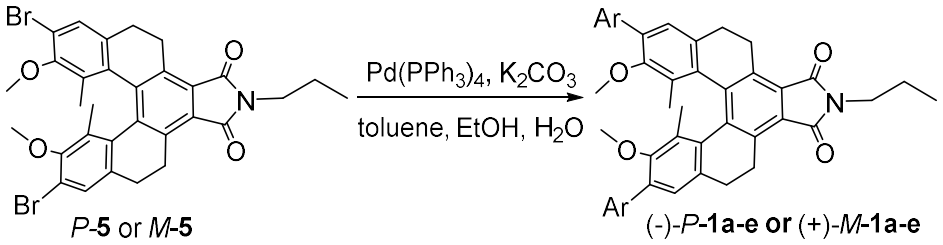

P-**5** or *M*-**5** (-)-*P*-**1a-e or** (+)-*M*-**1a-e**

To a mixture of compound *P*-**5** or *M*-**5** (639 mg, 1.0 mmol), K_2CO_3 (1.38 g, 10 mmol), and arylboronic acid (3.0 mmol) in toluene (30 mL), EtOH (30 mL), and degassed water (15 mL) under argon atmosphere was added catalytic amount of $Pd(PPh_3)_4$ (5 mol %), followed by strring at 75 °C for 12h under argon atmosphere. After the reaction mixture was cooled to room temperature, it was poured into ethyl acetate (100 mL). The organic layer was washed with saturated brine (3×100 mL), dried over anhydrous $MgSO_4$, and then concentrated in *vacuo*. The residue was purified by flash column chromatography with ethyl acetate, dichloromethane and petroleum ether (0.2:1:3, *v*/*v*/*v*) as eluent to give the corresponding pure enantiomers.

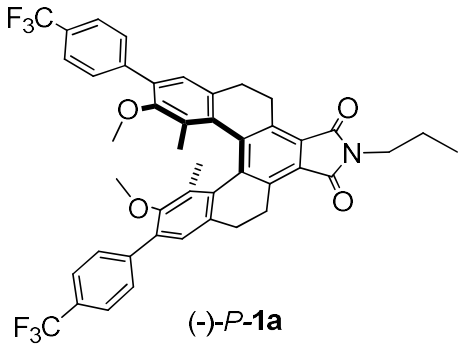

(-)-*P*-**1a**

Compound (–)-*P*-1a. According to the general method, (–)-*P*-**1a** (645 mg, 84%) was obtained as pale-yellow powder. R_f = 0.46 (EtOAc : DCM : PE, *v*/*v*/*v* ~ 0.2 : 1 : 3). M. p.: 157-158 °C. $[\alpha]^{25}_D$ = -32°. ^{1}H NMR (500 MHz, $CDCl_3$): δ 7.75–7.61 (m, 8H), 7.27 (s, 2H), 4.19–4.14 (m, 2H), 3.73–3.64 (m, 2H), 3.20 (s, 6H), 3.02–2.98 (m, 2H), 2.73 (td, *J* = 14.6, 3.9 Hz, 2H), 2.53 (td, *J* = 15.3, 3.9 Hz, 2H), 1.75 (h, *J* = 7.4 Hz, 2H), 1.33 (s, 6H), 1.00 (t, *J* = 7.4 Hz, 3H). ^{13}C NMR (126 MHz, $CDCl_3$): δ 169.0, 155.5, 141.9,

139.2, 139.0, 136.7, 136.1, 132.4, 129.9, 129.5, 129.2, 127.1, 125.35, 125.32, 125.29, 125.26, 125.23, 125.20, 123.2, 59.7, 39. 5, 29.7, 24.2, 22.0, 14.3, 11.5. ^{19}F NMR (565 MHz, $CDCl_3$): δ -62.46. HRMS (APCI): *m/z* calcd for $C_{45}H_{38}NO_4F_6$ $[M + H]^+$ 770.2700, found 770.2686.

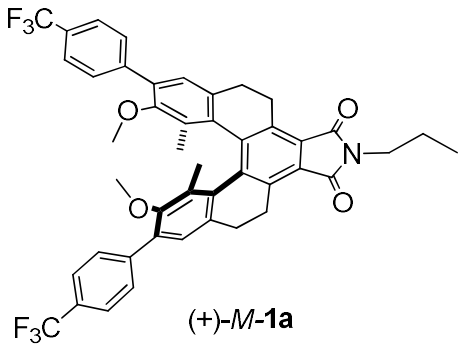

(+)-*M*-**1a**

Compound (+)-*M*-**1a.** According to the general method, (+)-*M*-**1a** (659 mg, 86%) was obtained as pale-yellow powder. R_f = 0.46 (EtOAc : DCM : PE, *v*/*v*/*v* ~ 0.2 : 1 : 3). M. p.: 157-158 °C. $[\alpha]^{25}_D$ = 28°. ^{1}H NMR (500 MHz, $CDCl_3$): δ 7.74–7.63 (m, 8H), 7.27 (s, 2H), 4.19–4.14 (m, 2H), 3.73–3.64 (m, 2H), 3.20 (s, 6H), 3.02–2.98 (m, 2H), 2.73 (td, *J* = 14.6, 3.9 Hz, 2H), 2.53 (td, *J* = 15.2, 4.1 Hz, 2H), 1.75 (h, *J* = 7.3 Hz, 2H), 1.33 (s, 6H), 1.00 (t, *J* = 7.4 Hz, 3H). ^{13}C NMR (126 MHz, $CDCl_3$) δ 169.0, 155.5, 141.9, 139.2, 139.0, 136.7, 136.1, 132.4, 129.9, 129.5, 129.21, 129.19, 127.1, 125.4, 125.33, 125.29, 125.26, 125.23, 125.20, 123.2, 59.7, 39.5, 29.7, 24.2, 22.0, 14.3, 11.5. ^{19}F NMR (565 MHz, $CDCl_3$): δ -62.44. HRMS (APCI): *m/z* calcd for $C_{45}H_{38}NO_4F_6$ $[M + H]^+$ 770.2700, found 770.2689.

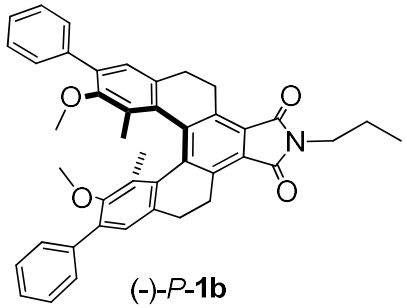

(-)-*P*-**1b**

Compound (–)-*P*-**1b.** According to the general method, (–)-*P*-**1b** (604 mg, 95%) was obtained as pale-yellow powder. R_f = 0.45 (EtOAc : DCM : PE, *v*/*v*/*v* ~ 0.2 : 1 : 3). M. p.: 124-127 °C. $[\alpha]^{25}_D$ = -40°. ^{1}H NMR (500 MHz, $CDCl_3$): δ 7.59–7.53 (m, 4H), 7.43–

7.39 (m, 4H), 7.36–7.31 (m, 2H), 4.14 (ddd, *J* = 15.5, 3.9, 2.2 Hz, 2H), 3.71–3.64 (m, 2H), 3.21 (s, 6H), 2.98 (ddd, *J* = 14.4, 4.2, 2.2 Hz, 2H), 2.72 (td, *J* = 14.6, 3.8 Hz, 2H), 2.53 (td, *J* = 15.2, 4.1 Hz, 2H), 1.75 (q, *J* = 7.4 Hz, 2H), 1.32 (s, 6H), 1.00 (t, *J* = 7.4 Hz, 3H). ^{13}C NMR (126 MHz, $CDCl_3$): δ 169.1, 155.4, 139.3, 139.0, 138.4, 136.4, 135.3, 133.8, 129.7, 128.9, 128.3, 127.22, 127.18, 125.1, 59.6, 39.4, 29.7, 24.2, 22.0, 14.3, 11.5. HRMS (APCI): *m/z* calcd for $C_{43}H_{40}NO_4$ $[M + H]^+$ 634.2952, found 634.2947.

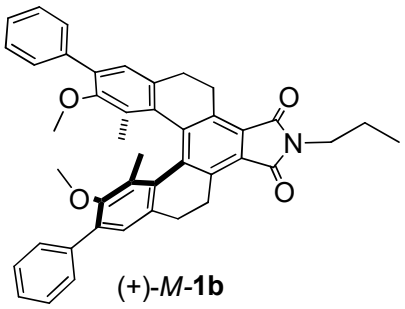

(+)-*M*-**1b**

Compound (+)-*M*-**1b.** According to the general method, (+)-*M*-**1b** (600 mg, 95%) was obtained as pale-yellow powder. R_f = 0.45 (EtOAc : DCM : PE, *v*/*v*/*v* ~ 0.2 : 1 : 3). M. p.: 124-126 °C. $[\alpha]^{25}_D$ = 48°. ^{1}H NMR (400 MHz, $CDCl_3$): δ 7.60–7.53 (m, 4H), 7.41 (t, *J* = 7.4 Hz, 4H), 7.37–7.31 (m, 2H), 4.16–4.13 (m, 2H), 3.68 (td, *J* = 7.1, 3.4 Hz, 2H), 3.21 (s, 6H), 2.98 (ddd, *J* = 14.3, 4.2, 2.2 Hz, 2H), 2.72 (td, *J* = 14.6, 3.8 Hz, 2H), 2.53 (td, *J* = 15.2, 4.1 Hz, 2H), 1.75 (h, *J* = 7.5 Hz, 2H), 1.32 (s, 6H), 1.01 (t, *J* = 7.4 Hz, 3H). ^{13}C NMR (126 MHz, $CDCl_3$): δ 169.1, 155.4, 139.3, 139.0, 138.3, 136.4, 135.3, 133.8, 129.7, 128.9, 128.3, 127.21, 127.18, 125.1, 59.6, 39.4, 29.7, 24.2, 22.0, 14.3, 11.5. HRMS (APCI): *m/z* calcd for $C_{43}H_{39}NO_4$ $[M]^+$ 633.2879, found 633.2870.

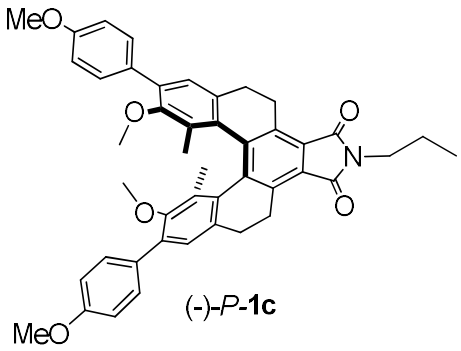

(-)-*P*-**1c**

Compound (–)-*P*-**1c.** According to the general method, (–)-*P*-**1c** (680 mg, 98%) was obtained as pale-yellow powder. R_f = 0.29 (EtOAc : DCM : PE, *v*/*v*/*v* ~ 0.2 : 1 : 3). M.

p.: 156-158 °C. $[\alpha]^{25}_D$ = -234°. ^{1}H NMR (500 MHz, $CDCl_3$): δ 7.56–7.48 (m, 4H), 7.23 (s, 2H), 7.01–6.91 (m, 4H), 4.15–4.11 (m, 2H), 3.86 (s, 6H), 3.74–3.63 (m, 2H), 3.20 (s, 6H), 2.98–2.94 (m, 2H), 2.71 (td, *J* = 14.5, 3.8 Hz, 2H), 2.52 (td, *J* = 15.2, 4.1 Hz, 2H), 1.75 (h, *J* = 7.4 Hz, 2H), 1.31 (s, 6H), 1.00 (t, *J* = 7.4 Hz, 3H). ^{13}C NMR (126 MHz, $CDCl_3$): δ 169.1, 158.9, 155.4, 139.4, 139.0, 136.4, 134.9, 133.4, 130.7, 130.0, 129.7, 126.9, 125.0, 113.7, 59.4, 55.3, 39.4, 29.7, 24.2, 22.0, 14.2, 14.1, 11.5. HRMS (APCI): *m/z* calcd for $C_{45}H_{44}NO_6$ $[M + H]^+$ 694.3163, found 694.3149.

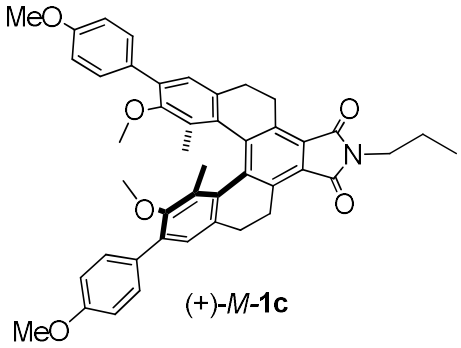

(+)-*M*-**1c**

Compound (+)-*M*-**1c.** According to the general method, (+)-*M*-**1c** (673 mg, 97%) was obtained as pale-yellow powder. R_f = 0.29 (EtOAc : DCM : PE, *v*/*v*/*v* ~ 0.2 : 1 : 3). M. p.: 156-158 °C. $[\alpha]^{25}_D$ = 162°. ^{1}H NMR (500 MHz, $CDCl_3$): δ 7.51 (d, *J* = 8.7 Hz, 4H), 7.23 (s, 2H), 6.95 (d, *J* = 8.7 Hz, 4H), 4.15–4.11 (m, 2H), 3.86 (s, 6H), 3.72–3.63 (m, 2H), 3.20 (s, 6H), 2.98–2.94 (m, 2H), 2.71 (td, *J* = 14.5, 3.8 Hz, 2H), 2.52 (td, *J* = 15.2, 4.1 Hz, 2H), 1.75 (h, *J* = 7.3 Hz, 2H), 1.31 (s, 6H), 1.00 (t, *J* = 7.4 Hz, 3H). ^{13}C NMR (126 MHz, $CDCl_3$): δ 169.1, 158.9, 155.4, 139.4, 139.0, 136.4, 134.9, 133.4, 130.7, 130.0, 129.7, 126.9, 125.0, 113.7, 59.4, 55.3, 39.4, 29.7, 24.2, 22.0, 14.2, 11.5. HRMS (APCI): *m/z* calcd for $C_{45}H_{44}NO_6$ $[M + H]^+$ 694.3163, found 694.3152.

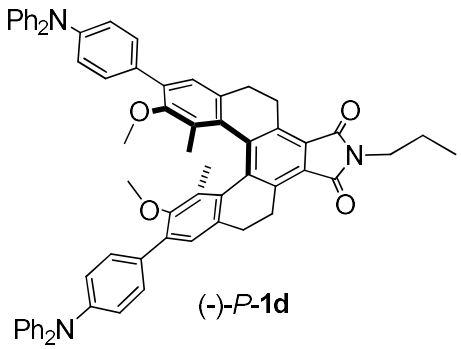

(-)-*P*-**1d**

Compound (–)-*P*-**1d.** According to the general method, (–)-*P*-**1d** (960 mg, 99%) was obtained as pale-yellow powder. R_f = 0.46 (EtOAc : DCM : PE, *v*/*v*/*v* ~ 0.2 : 1 : 3). M. p.: 183-186 °C. $[\alpha]^{25}_D$ = -221°. ^{1}H NMR (500 MHz, $CDCl_3$): δ 7.48–7.42 (m, 4H), 7.29–7.27 (m, 4H), 7.25 (s, 2H), 7.19–7.06 (m, 12H), 7.06–7.01 (m, 4H), 4.16–4.11 (m, 2H), 3.72–3.62 (m, 2H), 3.27 (s, 6H), 2.98–2.94 (m, 2H), 2.70 (td, *J* = 14.6, 3.7 Hz, 2H), 2.52 (td, *J* = 15.2, 4.1 Hz, 2H), 1.78–1.71 (m, 2H), 1.30 (s, 6H), 1.00 (t, *J* = 7.4 Hz, 3H). ^{13}C NMR (126 MHz, $CDCl_3$) δ 169.1, 155.4, 147.6, 147.0, 139.3, 139.0, 136.4, 134.9, 133.3, 132.2, 129.7, 129.6, 129.3, 126.8, 125.0, 124.5, 123.3, 122.9, 59.5, 39.4, 29.7, 24.3, 22.0, 14.3, 11.5. HRMS (APCI): *m/z* calcd for $C_{67}H_{58}N_3O_4$ $[M + H]^+$ 968.4422, found 968.4415.

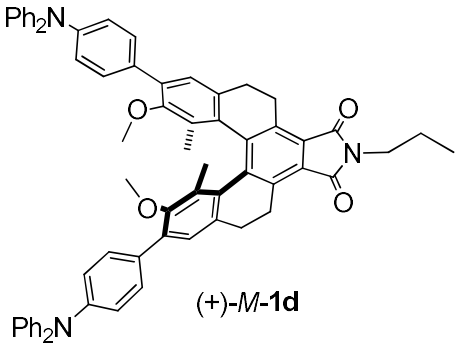

(+)-*M*-**1d**

Compound (+)-*M*-**1d.** According to the general method, (+)-*M*-**1d** (911 mg, 94%) was obtained as pale-yellow powder. R_f = 0.46 (EtOAc : DCM : PE, *v*/*v*/*v* ~ 0.2 : 1 : 3). M. p.: 183-186 °C. $[\alpha]^{25}_D$ = 207°. ^{1}H NMR (500 MHz, $CDCl_3$): δ 7.45 (d, *J* = 8.3 Hz, 4H), 7.28 (d, *J* = 7.7 Hz, 5H), 7.25 (s, 2H), 7.12 (dd, *J* = 16.5, 8.1 Hz, 11H), 7.03 (t, *J* = 7.3 Hz, 4H), 4.13 (dt, *J* = 15.6, 2.9 Hz, 2H), 3.67 (td, *J* = 6.9, 4.8 Hz, 2H), 3.27 (s, 6H), 3.00–2.92 (m, 2H), 2.70 (td, *J* = 14.6, 3.8 Hz, 2H), 2.52 (td, *J* = 15.3, 4.1 Hz, 2H), 1.74 (h, *J* = 7.4 Hz, 2H), 1.30 (s, 6H), 1.00 (t, *J* = 7.4 Hz, 3H). ^{13}C NMR (126 MHz, $CDCl_3$): δ 169.1, 155.4, 147.7, 147.0, 139.3, 139.0, 136.4, 134.9, 133.3, 132.2, 129.7, 129.6, 129.3, 126.8, 125.0, 124.5, 123.3, 123.0, 59.5, 39.4, 29.7, 24.2, 22.0, 14.3, 11.5. HRMS (APCI): *m/z* calcd for $C_{67}H_{58}N_3O_4$ $[M + H]^+$ 968.4422, found 968.4420.

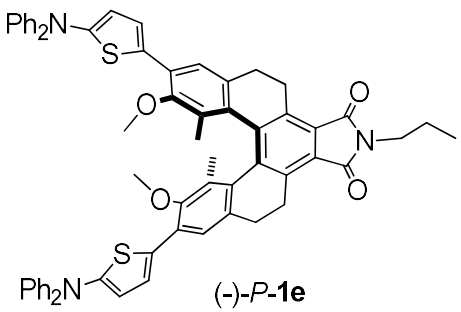

(-)-*P*-**1e**

Compound (–)-*P*-**1e.** According to the general method, (–)-*P*-**1e** (890 mg, 91%) was obtained as pale-yellow powder. R_f = 0.46 (EtOAc : DCM : PE, *v*/*v*/*v* ~ 0.2 : 1 : 3). M. p.: 132-133 °C. $[\alpha]^{25}_D$ = -213°. ^{1}H NMR (500 MHz, $CDCl_3$): δ 7.48–7.40 (m, 4H), 7.28–7.26 (m, 4H), 7.25 (m, 2H), 7.18–7.07 (m, 12H), 7.06–7.01 (m, 4H), 4.15–4.11 (m, 2H), 3.67 (td, *J* = 7.1, 4.9 Hz, 2H), 3.26 (s, 6H), 2.98–2.94 (m, 2H), 2.70 (td, *J* = 14.6, 3.6 Hz, 2H), 2.52 (td, *J* = 15.2, 4.1 Hz, 2H), 1.74 (h, *J* = 7.4 Hz, 2H), 1.29 (s, 6H), 1.00 (t, *J* = 7.4 Hz, 3H). ^{13}C NMR (126 MHz, $CDCl_3$): δ 169.0, 154.1, 152.6, 147.7, 139.0, 138.9, 136.6, 134.8, 132.0, 129.9, 129.2, 126.7, 124.9, 124.3, 123.9, 123.1, 122. 9, 120.0, 59.5, 39.4, 29.8, 24.2, 22.0, 14.2, 11.5. HRMS (APCI): *m/z* calcd for $C_{63}H_{54}N_3O_4S_2$ $[M + H]^+$ 980.3550, found 980.3553.

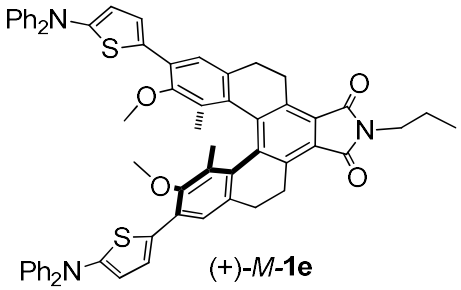

(+)-*M*-**1e**

Compound (+)-*M*-**1e.** According to the general method, (+)-*M*-**1e** (850 mg, 87%) was obtained as pale-yellow powder. R_f = 0.46 (EtOAc : DCM : PE, *v*/*v*/*v* ~ 0.2 : 1 : 3). M. p.: 132-135 °C. $[\alpha]^{25}_D$ = 265°. ^{1}H NMR (500 MHz, $CDCl_3$): δ 7.45 (s, 2H), 7.31–7.27 (m, 4H), 7.27 (s, 2H), 7.25 (d, *J* = 2.3 Hz, 4H), 7.19–7.18 (m, 8H), 7.04 (t, *J* = 7.3 Hz, 4H), 6.64 (d, *J* = 3.9 Hz, 2H), 4.13–4.10 (m, 2H), 3.66 (h, *J* = 6.5, 5.7 Hz, 2H), 3.39 (s, 6H), 2.94 (dt, *J* = 14.3, 3.2 Hz, 2H), 2.67 (td, *J* = 14.6, 3.9 Hz, 2H), 2.48 (td, *J* = 15.3, 4.1 Hz, 2H), 1.73 (q, *J* = 7.4 Hz, 2H), 1.30 (s, 6H), 0.99 (t, *J* = 7.1 Hz, 3H). ^{13}C NMR (126 MHz, $CDCl_3$): δ 169.0, 154.1, 152.6, 147.7, 139.1, 138.9, 136.6, 134.8, 132.0, 129.9, 129.2, 126.7, 124.9, 124.3, 123.9, 123.1, 122.9, 120.0, 59.5, 39.4, 29.8, 24.2,

22.0, 14.2, 11.5. HRMS (APCI): *m/z* calcd for $C_{63}H_{53}N_3O_4S_2$ $[M]^+$ 979.3477, found 979.3483.

3. Crystal structures and crystal data

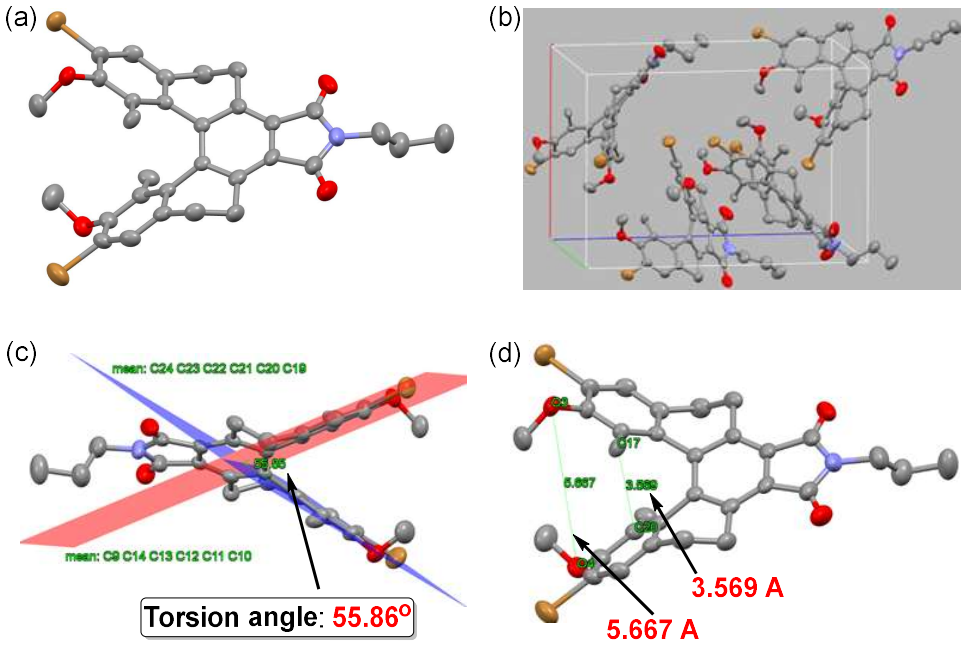

Fig. S1. (a) X-ray crystal structure, (b) crystal packing, (c) torsion angle, and (d) distance of methoxyl groups and methyl groups of *P*-**5**.

Table S1. Crystal data and structure refinement for *P*-**5** (CCDC 1465234)

Empirical formula	$C_{31}H_{29}Br_2NO_4$
Formula weight	639.37
Temperature	173.1500 K
Wavelength	0.71073 Å
Crystal system	Tetragonal
Space group	P 43
Unit cell dimensions	a = 12.3390(3) Å α = 90°. b = 12.3390(7) Å β = 90°. c = 18.0683(7) Å γ = 90°.
Volume	2750.92(17) $Å^3$
Z	4
Density (calculated)	1.544 Mg/m^3
Absorption coefficient	2.984 mm^{-1}
F(000)	1296
Crystal size	0.21 x 0.17 x 0.13 mm^3

Theta range for data collection	1.650 to 27.484°.
Index ranges	-16<=h<=15, -16<=k<=15, -20<=l<=23
Reflections collected	17959
Independent reflections	5824 [R(int) = 0.0419]
Completeness to theta = 26.000°	100.0 %
Absorption correction	Semi-empirical from equivalents
Max. and min. transmission	1.0000 and 0.6689
Refinement method	Full-matrix least-squares on F^2
Data / restraints / parameters	5824 / 1 / 348
Goodness-of-fit on F^2	1.056
Final R indices [I>2sigma(I)]	R1 = 0.0534, wR2 = 0.1270
R indices (all data)	R1 = 0.0585, wR2 = 0.1321
Absolute structure parameter	-0.008(7)
Extinction coefficient	n/a
Largest diff. peak and hole	0.754 and -0.460 e.Å^{-3}

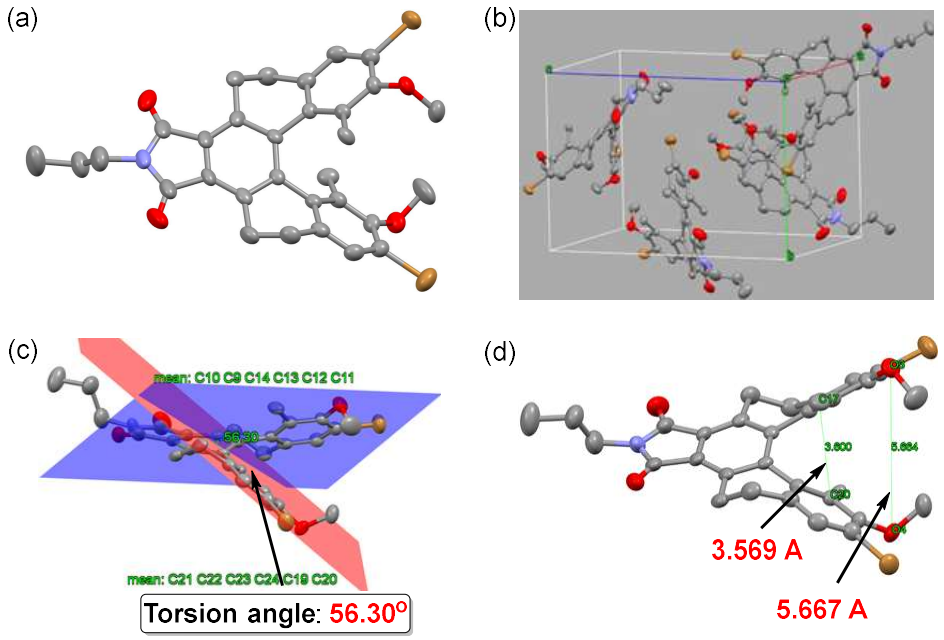

Fig. S2. (a) X-ray crystal structure, (b) crystal packing, (c) torsion angle, and (d) distance of methoxyl groups and methyl groups of *M*-**5**.

Table S2. Crystal data and structure refinement for *M*-**5** (CCDC 1465240)

Empirical formula	$C_{31}H_{29}Br_2NO_4$
Formula weight	639.37
Temperature	173.1500 K
Wavelength	0.71073 Å

Crystal system	Tetragonal
Space group	P 41
Unit cell dimensions	a = 12.347(3) Å α = 90°. b = 12.347(3) Å β = 90°. c = 18.073(4) Å γ = 90°.
Volume	2755.1(13) $Å^3$
Z	4
Density (calculated)	1.541 Mg/m^3
Absorption coefficient	2.980 mm^{-1}
F(000)	1296
Crystal size	0.31 x 0.11 x 0.04 mm^3
Theta range for data collection	1.649 to 27.471°.
Index ranges	-16<=h<=16, -16<=k<=16, -23<=l<=23
Reflections collected	31763
Independent reflections	6298 [R(int) = 0.0733]
Completeness to theta = 26.000°	100.0 %
Absorption correction	Semi-empirical from equivalents
Max. and min. transmission	1.0000 and 0.6305
Refinement method	Full-matrix least-squares on F^2
Data / restraints / parameters	6298 / 1 / 348
Goodness-of-fit on F^2	1.100
Final R indices [I>2sigma(I)]	R1 = 0.0645, wR2 = 0.1466
R indices (all data)	R1 = 0.0707, wR2 = 0.1510
Absolute structure parameter	0.008(7)
Extinction coefficient	n/a
Largest diff. peak and hole	0.794 and -0.450 $e.Å^{-3}$

4. HPLC charts

Optical resolution conditions

Table S3. Semi-preparative supercritical fluid chromatography (SFC) conditions

Column	:	Chiralpak® IC
Column size	:	0.46 cm I.D. × 15 cm L
Injection	:	6.0 μl

Mobile phase	:	CO_2/MeOH/DCM=40/30/30（*v*/*v*/*v*)
Flow rate	:	2.0 mL/min
Wave length	:	UV 254 nm
Temperature	:	35 ºC

Analysis of the enantiomer excess of 5

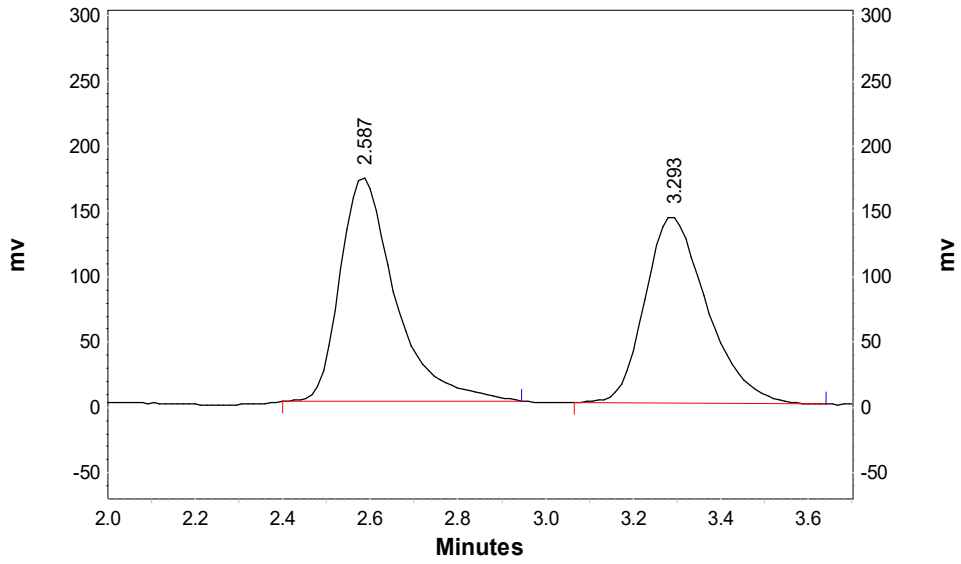

Fig. S3. SFC profile of *rac*-**5**.

Table S4. The summary of SFC profiles of *rac*-**5**.

Peak	Ret. Time	Area	Area%	T. Plate	Height	Height %
P-**5**	2.587	1505133	51.60	171457	54.60	2.587
M-**5**	3.293	1411973	48.40	142572	45.40	3.293

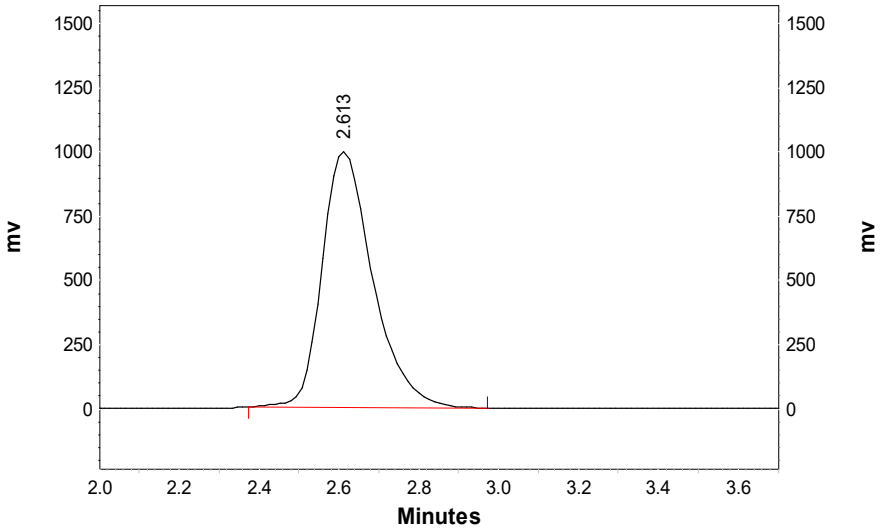

Fig. S4. SFC profile of *P*-**5**.

Table S5. The summary of SFC profiles of *P*-**5**.

Peak	Ret. Time	Area	Area%	T. Plate	Height	Height %
P-**5**	2.613	8805505	100.00	993952	100.00	2.613
***ee* value of *P*-5: > 99.9%**						

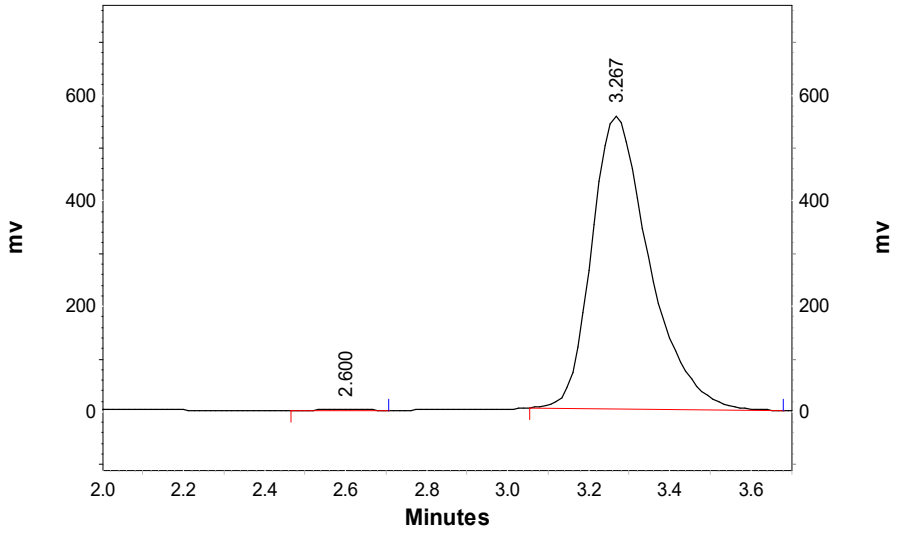

Fig. S5. SFC profile of *M*-**5**.

Table S6. The summary of SFC profiles of *M*-**5**.

Peak	Ret. Time	Area	Area %	Height	Height %	Ret. Time
P-**5**	2.600	15772	0.29	2282	0.41	2.600
M-**5**	3.267	5480162	99.71	553741	99.59	3.267
***ee* value of *M*-5: 99.4%**						

Racemization kinetic experiments

Time-dependent HPLC measurements were performed to determine the activation parameters for the racemization.[2] *M*-**5** (20 mg) was dissolved in diethylene glycol dibutyl ether (8 mL). The solution was heated at 423 K continuously, and 0.5 mL of this solution was sampled for different time inervals to analyzed immediately by HPLC (Daicel Chiralpak IC, 4.6 mm × 250 mm) to determine the initial enantiomeric excess depending on time. The HPLC measurements were performed keeping the column at 4 ^{o}C.

A first order kinetic equation was obtained by representation of ln(A/A_0) against time, where A was the concentration of the *ee* and A_0 was the initial concentration, and the k was reaction rate constant. The Gibbs' free energy barrier to racemization ($\Delta G^{\ddagger}$) of chiral synthon *M*-**5**, was determined according to the Eyring equation (Eq. S1)

$$\Delta G^{\ddagger} = -RT\ln(\frac{k_T \cdot h}{\kappa \cdot k_B \cdot T}) \qquad \text{Eq. S1}$$

Where R is gas constant (R = 8.31441 J·K^{-1}·mol^{-1}), T is absolute temperature (K), κ is transition factor (κ = 0.5), h is Planck's constant (h = 6.62606896 × 10^{-34} J·s), k_T is reaction rate constant, and k_B is Boltzamann's constant (k_B = 1.380662 × 10^{-23} J·K^{-1}).

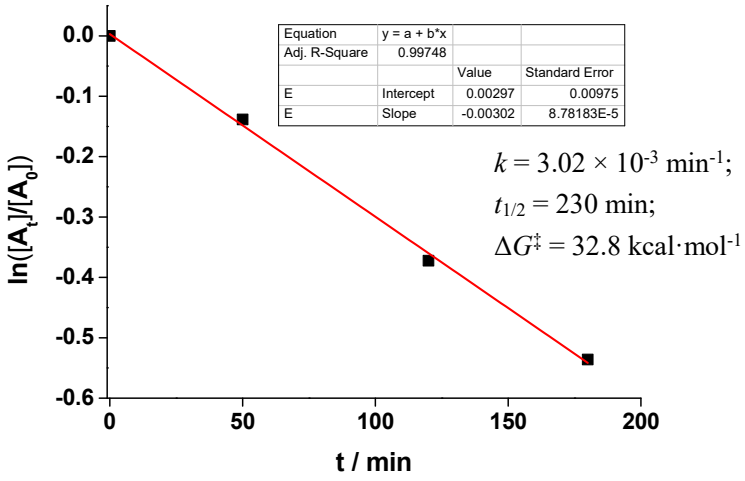

Fig. S6. ln(A/A_0) = k (time, min) plot for *M*-**5** at 423 K.

Analysis of the enantiomer excess of (–)-*P*-1a-e and (+)-*M*-1a-e

HPLC Analysis Conditions:

Column: Chiralpak® IC 5 μm, 4.6 mm × 250 mm

Mobile phase: hexane: dichloromethane = 50:50

Flow rate: 0.5 mL/min

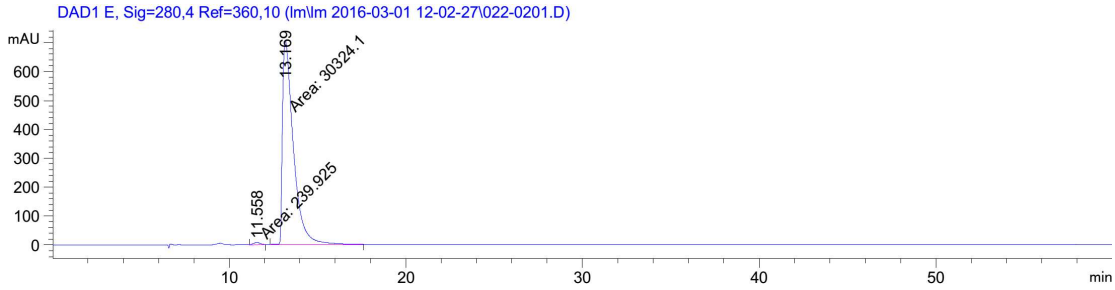

Fig. S7. HPLC profile of (−)-*P*-**1a**.

Table S7. The summary of HPLC profiles of (−)-*P*-**1a**.

Compound	Peak	RetTime (min)	Area (mAU·s)	Area %	ee value
(−)-*P*-**1a**	1	11.56	335.5	0.73	98.5 %
	2	13.17	4.55×10^4	99.27	

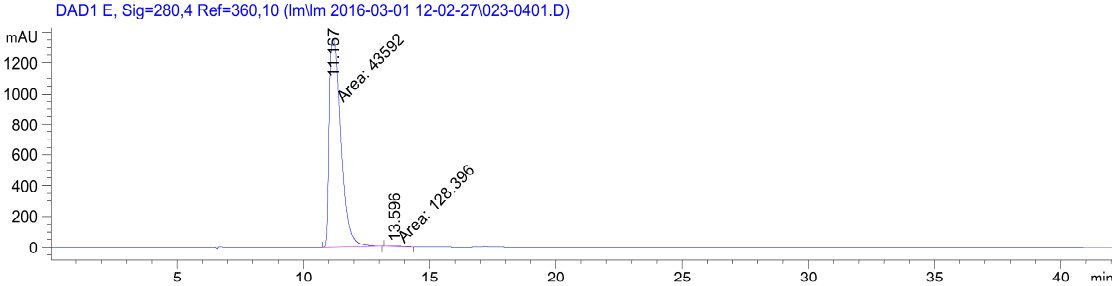

Fig. S8. HPLC profile of (+)-*M*-**1a**.

Table S8. The summary of HPLC profiles of (+)-*M*-**1a**.

Compound	Peak	RetTime (min)	Area (mAU·s)	Area %	ee value
(+)-*M*-**1a**	1	11.17	4.36×10^4	99.71	99.4 %
	2	13.60	128.40	0.29	

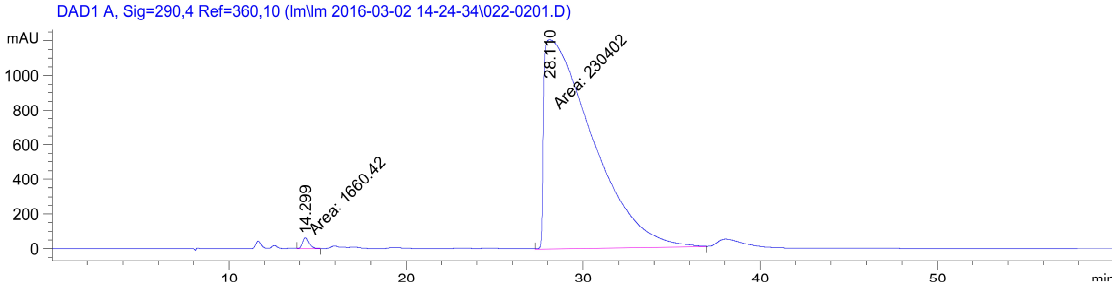

Fig. S9. HPLC profile of (−)-*P*-**1b**.

Table S9. The summary of HPLC profiles of (−)-*P*-**1b**.

Compound	Peak	RetTime (min)	Area (mAU·s)	Area %	ee value
(−)-*P*-**1b**	1	14.30	1660.42	0.72	98.6 %
	2	28.11	2.30×10^5	99.28	

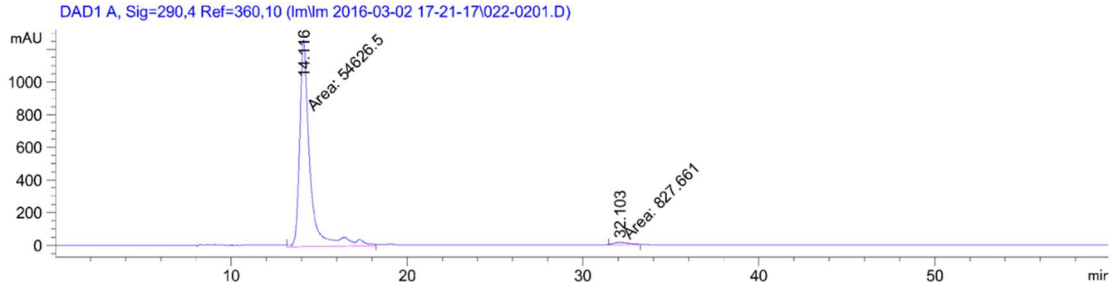

Fig. S10. HPLC profile of (+)-*M*-**1b**.

Table S10. The summary of HPLC profiles of (+)-*M*-**1b**.

Compound	Peak	RetTime (min)	Area (mAU·s)	Area %	ee value
(+)-*M*-**1b**	1	14.12	5.46×10^4	98.51	97.0 %
	2	32.10	827.66	1.49	

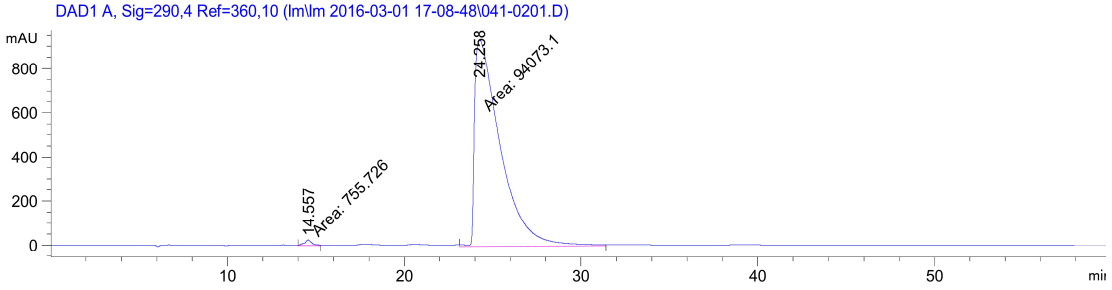

Fig. S11. HPLC profile of (−)-*P*-**1c**.

Table S11. The summary of HPLC profiles of (−)-*P*-**1c**.

Compound	Peak	Ret Time (min)	Area (mAU·s)	Area %	ee value
(−)-*P*-**1c**	1	14.56	755.73	0.80	98.4 %
	2	24.26	9.41×10^4	99.20	

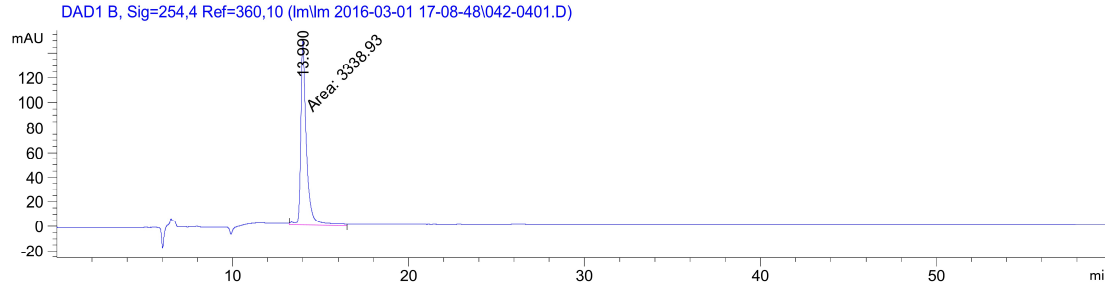

Fig. S12. HPLC profile of (+)-*M*-**1c**.

Table S12. The summary of HPLC profiles of (+)-*M*-**1c**.

Compound	Peak	RetTime (min)	Area (mAU·s)	Area %	ee value
(+)-*M*-**1c**	1	13.99	3338.93	100	> 99.9 %

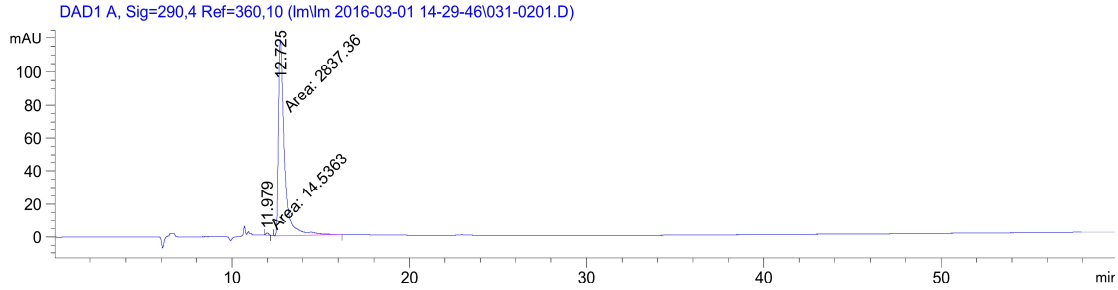

Fig. S13. HPLC profile of (−)-*P*-**1d**.

Table S13. The summary of HPLC profiles of (−)-*P*-**1d**.

Compound	Peak	RetTime (min)	Area (mAU·s)	Area %	ee value
(−)-*P*-**1d**	1	11.98	14.54	0.51	99.0 %
	2	12.73	2837.36	99.49	

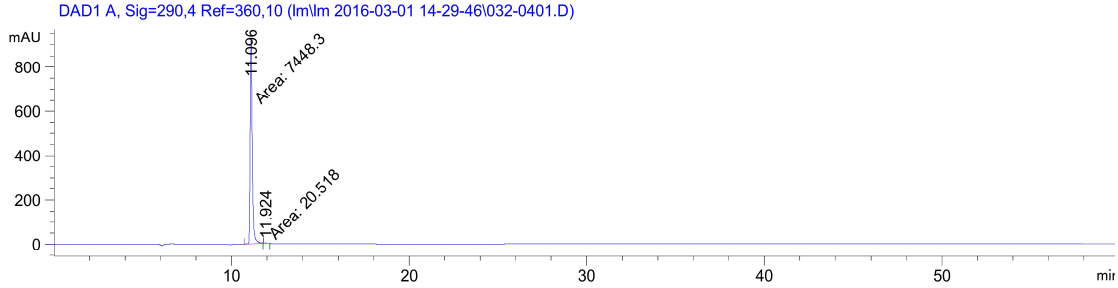

Fig. S14. HPLC profile of (+)-*M*-**1d**.

Table S14. The summary of HPLC profiles of (+)-*M*-**1d**.

Compound	Peak	RetTime (min)	Area (mAU·s)	Area %	ee value

(+)-*M*-**1d**	1	11.10	7448.30	99.73	99.5 %
	2	11.92	20.52	0.27	

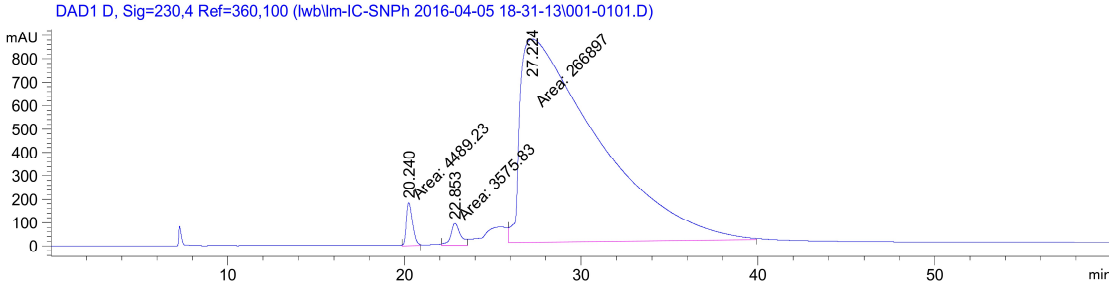

Fig. S15. HPLC profile of (−)-*P*-**1e**.

Table S15. The summary of HPLC profiles of (−)-*P*-**1e**.

Compound	Peak	RetTime (min)	Area (mAU·s)	Area %	ee value
(–)-*P*-**1e**	1	22.85	3575.83	1.30	98.7 %
	2	27.22	2.67×10^6	97.07	

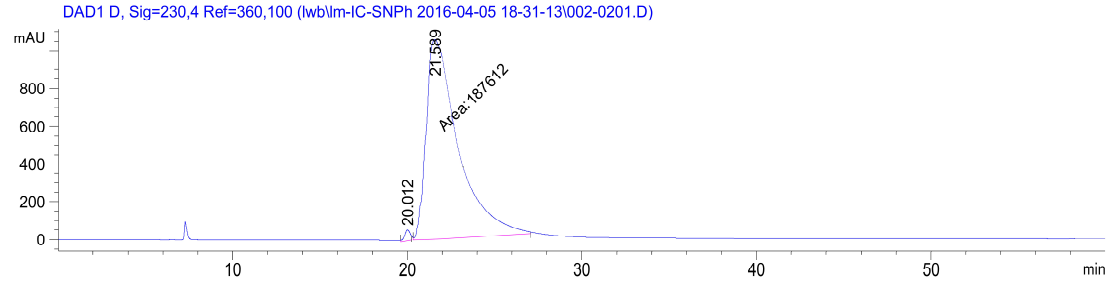

Fig. S16. HPLC profile of (+)-*M*-**1e**.

Table S16. The summary of HPLC profiles of (+)-*M*-**1e**.

Compound	Peak	RetTime (min)	Area (mAU·s)	Area %	ee value
(+)-*M*-**1e**	1	21.59	1.88×10^5	99.35	> 99 %

5. Photophysical properties of enantiomers 1a-e

UV-vis absorption and fluorescence spectra

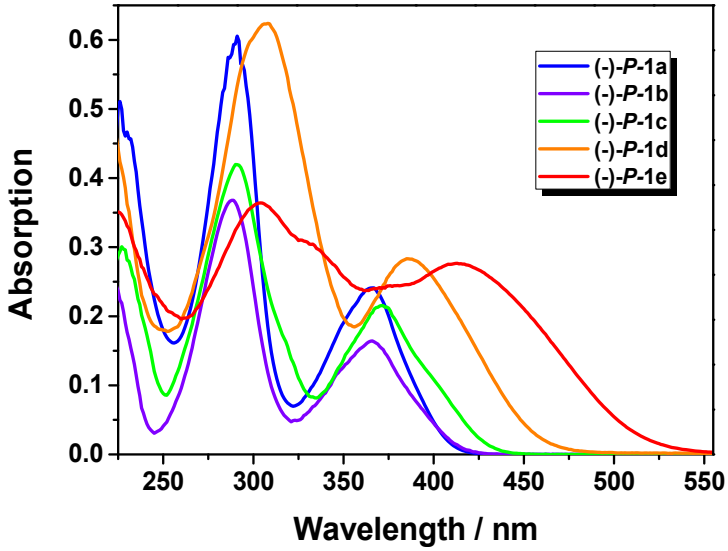

Fig. S17. UV/Vis spectra of (−)-*P*-**1a-e** in THF at room temperature (c = 1.0 × 10^{-5} M).

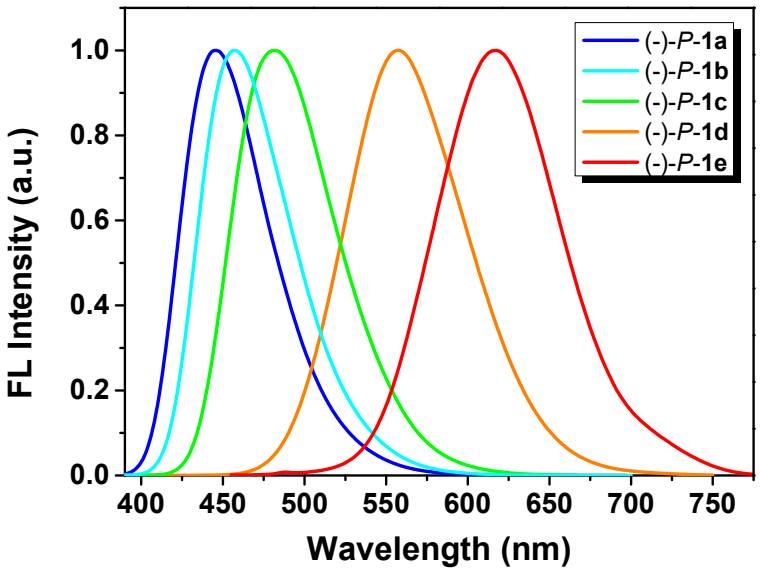

Fig. S18. Full-color emission spectra of (−)-*P*-**1a-e** in THF at room temperature (c = 1.0 × 10^{-5} M).

CD Spectra at different temperatures

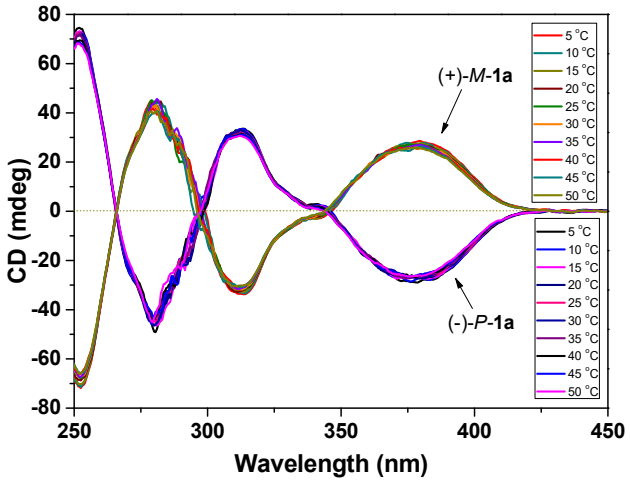

Fig. S19. CD spectra of (–)-*P*-**1a** and (+)-*M*-**1a** in THF (c = 5.0 × 10^{-5} M) at different temperatures.

Absorption dissymmetry factors (g_{abs}) and luminescence dissymmetry factors (g_{lum}) of the enantiomers 1a-e

Table S17. Absorption dissymmetry factor (g_{abs}) of (–)-*P*-**1a-e** and (+)-*M*-**1a-e**

Enantiomers	g_{abs}	Enantiomers	g_{abs}
(–)-*P*-**1a**	-1.55×10^{-3} (373 nm)	(+)-*M*-**1a**	1.52×10^{-3} (373 nm)
(–)-*P*-**1b**	-1.33×10^{-3} (375 nm)	(+)-*M*-**1b**	1.42×10^{-3} (375 nm)
(–)-*P*-**1c**	-1.35×10^{-3} (388 nm)	(+)-*M*-**1c**	1.36×10^{-3} (388 nm)
(–)-*P*-**1d**	-1.31×10^{-3} (411 nm)	(+)-*M*-**1d**	1.30×10^{-3} (411 nm)
(–)-*P*-**1e**	-3.53×10^{-4} (414 nm)	(+)-*M*-**1e**	3.59×10^{-4} (414 nm)

Table S18. Luminescence dissymmetry factors (g_{lum}) of (–)-*P*-**1a-e** and (+)-*M*-**1a-e**

Enantiomers	g_{lum} (×10^{-3})	Enantiomers	g_{lum}(×10^{-3})
(–)-*P*-**1a**	-1.2 (445 nm)	(+)-*M*-**1a**	1.3 (445 nm)
(–)-*P*-**1b**	-1.5 (460 nm)	(+)-*M*-**1b**	1.4 (460 nm)
(–)-*P*-**1c**	-0.8 (490 nm)	(+)-*M*-**1c**	1.0 (490 nm)
(–)-*P*-**1d**	-0.8 (558 nm)	(+)-*M*-**1d**	0.7 (554 nm)
(–)-*P*-**1e**	-0.2 (617 nm)	(+)-*M*-**1e**	0.4 (623 nm)

References

1. Y. Shen, H.-Y. Lu, C.-F. Chen, *Angew. Chem., Int. Ed.*, 2014, ***53***, 4648-4651.

2. K. Yamamoto, M. Okazumi, H. Suemune and K. Usui, *Org. Lett.*, 2013, **15**, 1806-1809.

6. Copies of ^{1}H NMR and ^{13}C NMR spectra of new compounds

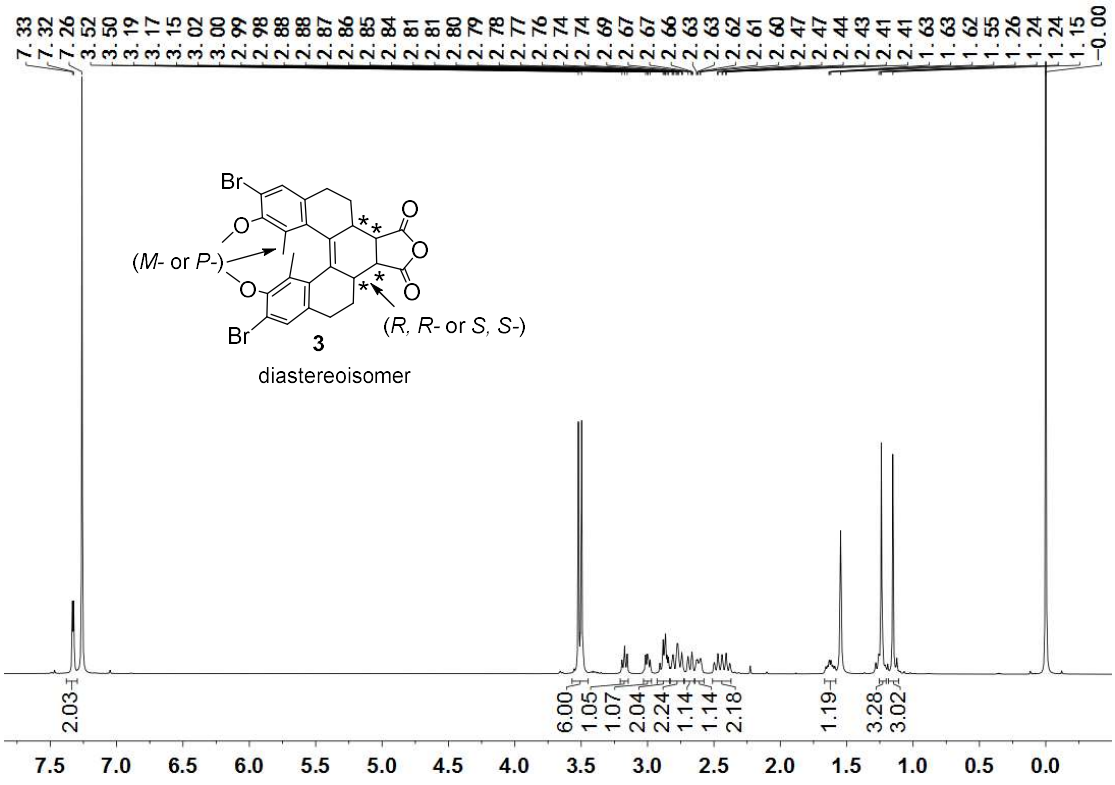

Fig. S20. ^{1}H NMR spectrum (500 MHz, $CDCl_3$) of *diastereoisomer*-**3**.

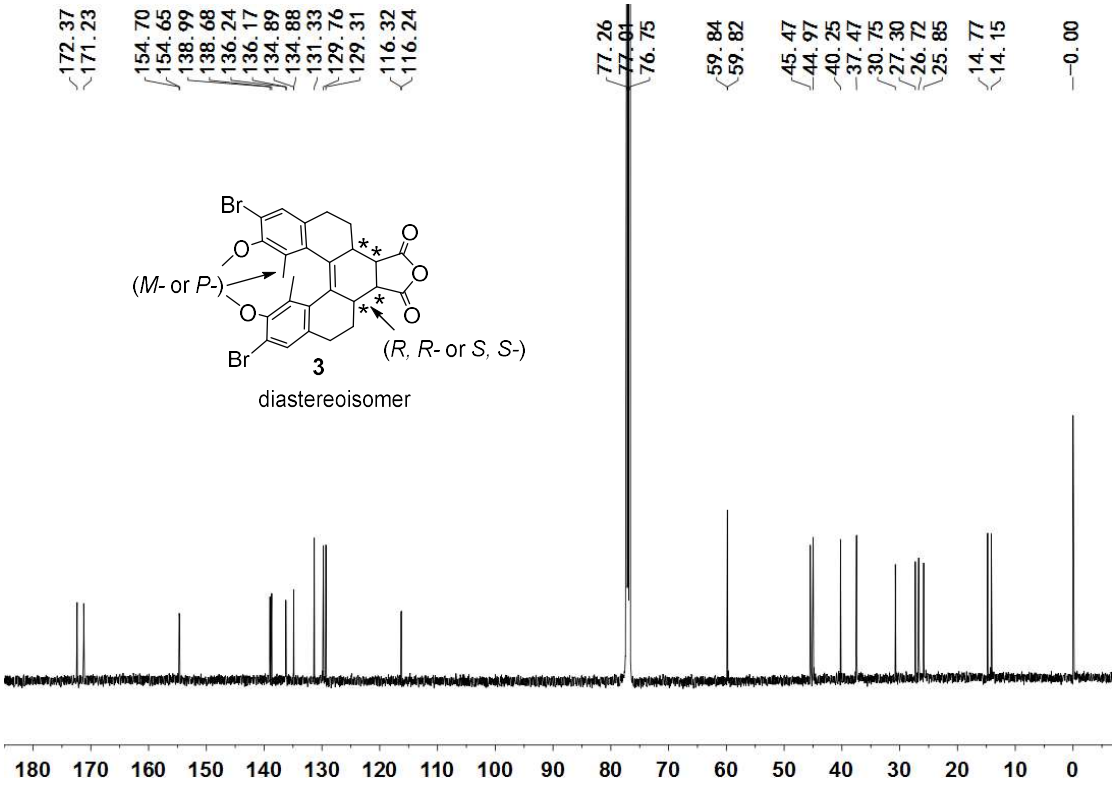

Fig. S21. ^{13}C NMR spectrum (126 MHz, $CDCl_3$) of *diastereoisomer*-**3**.

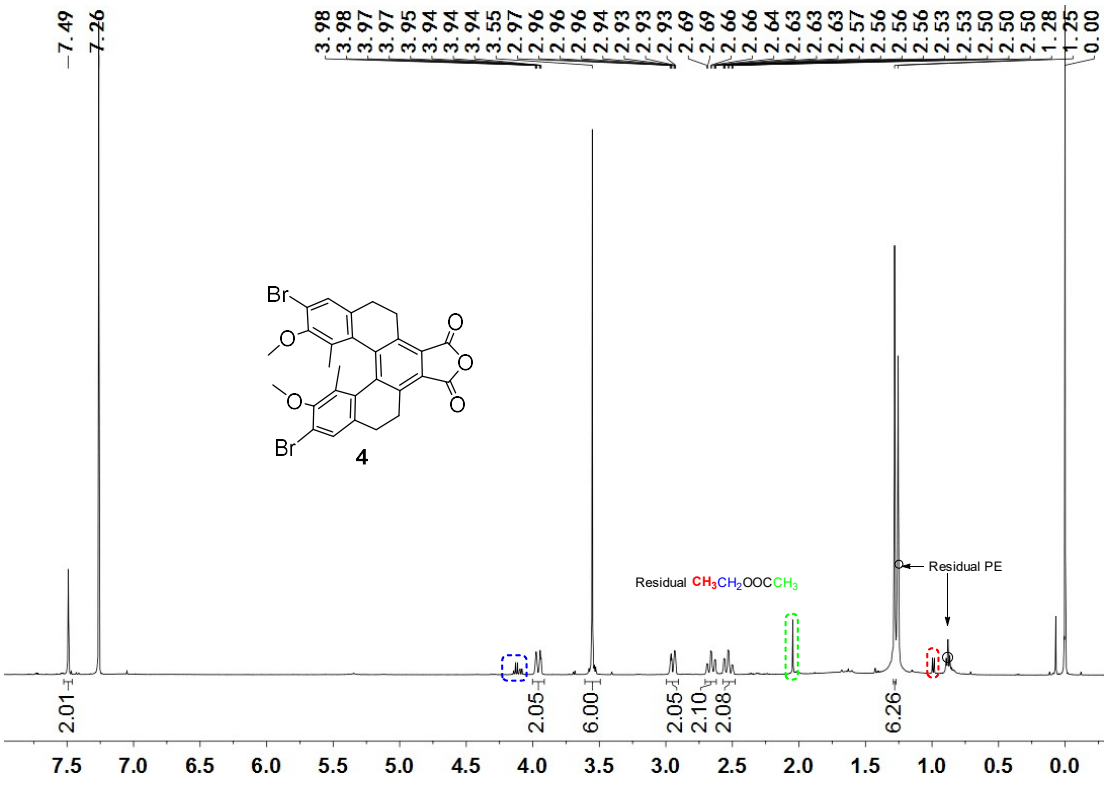

Fig. S22. ^{1}H NMR spectrum (500 MHz, $CDCl_3$) of **4**.

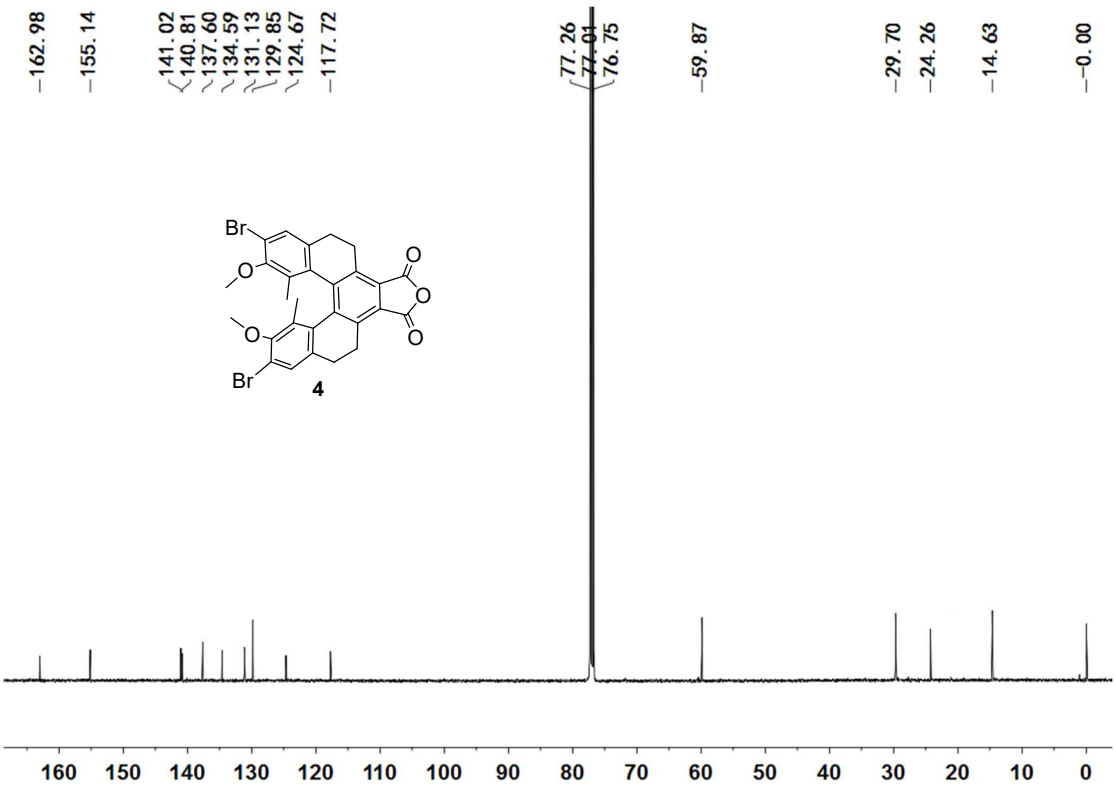

Fig. S23. ^{13}C NMR spectrum (126 MHz, $CDCl_3$) of **4**.

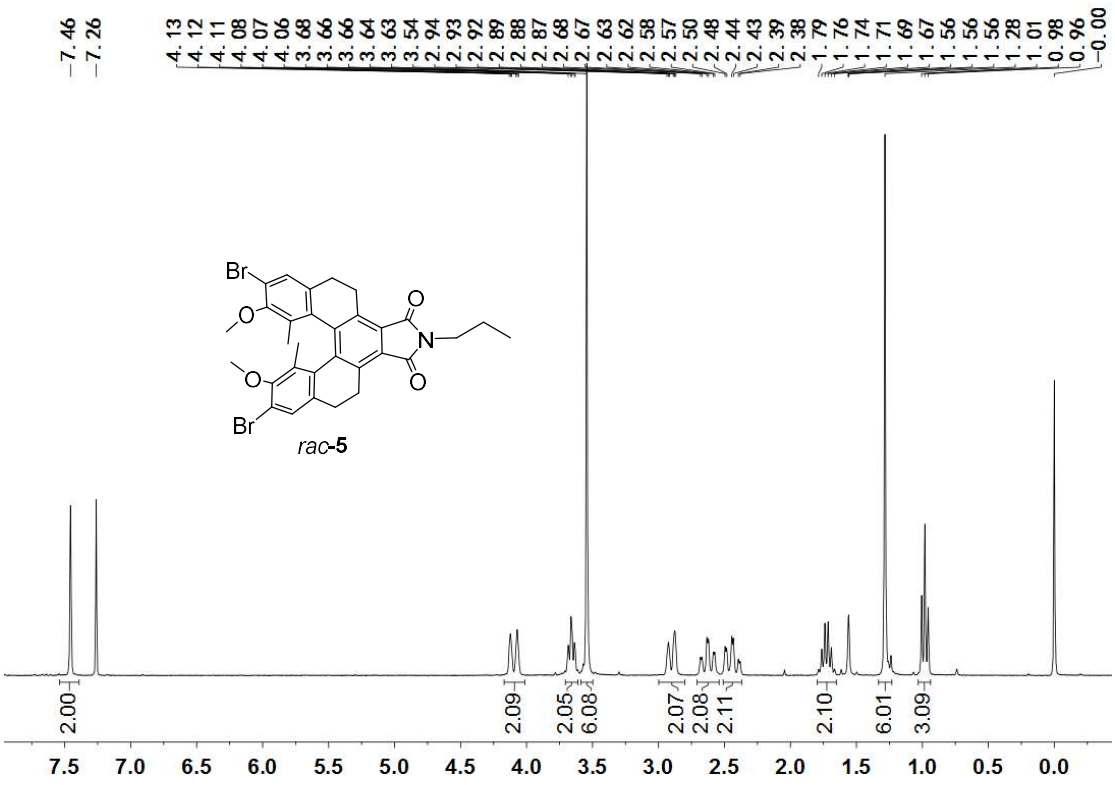

Fig. S24. ^{1}H NMR spectrum (300 MHz, $CDCl_3$) of *rac*-**5**.

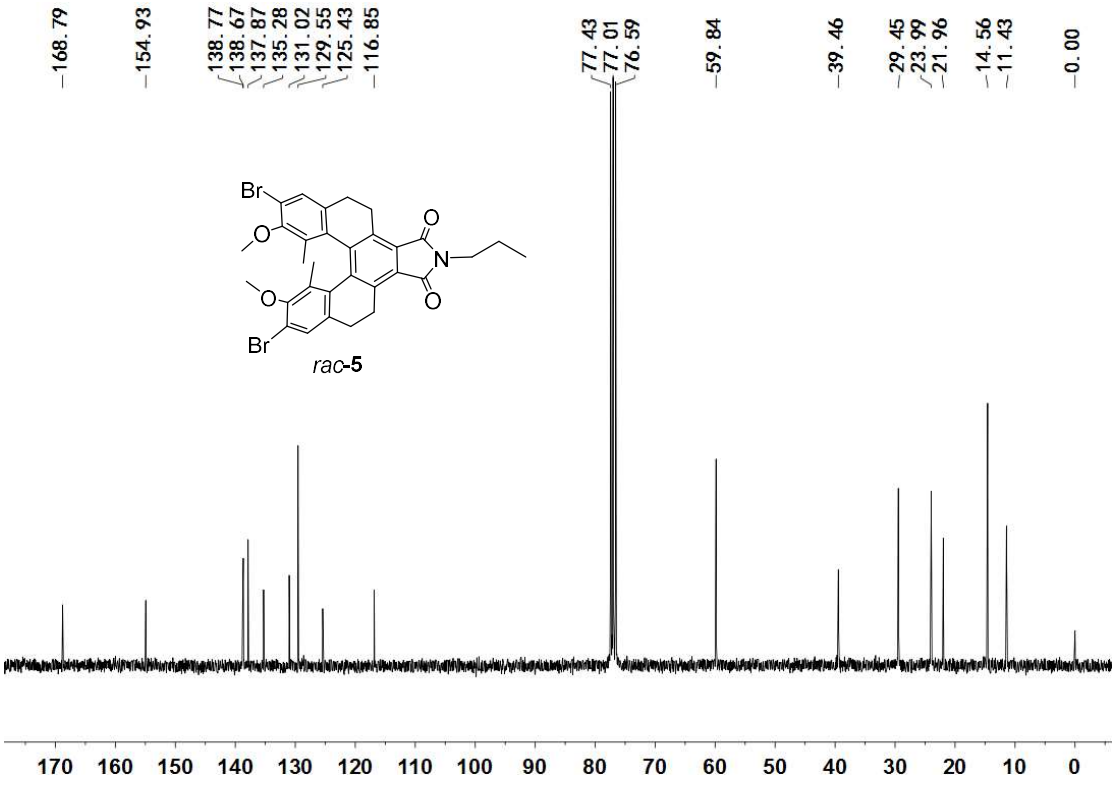

Figure 25. ^{13}C NMR spectrum (75 MHz, $CDCl_3$) of *rac*-**5**.

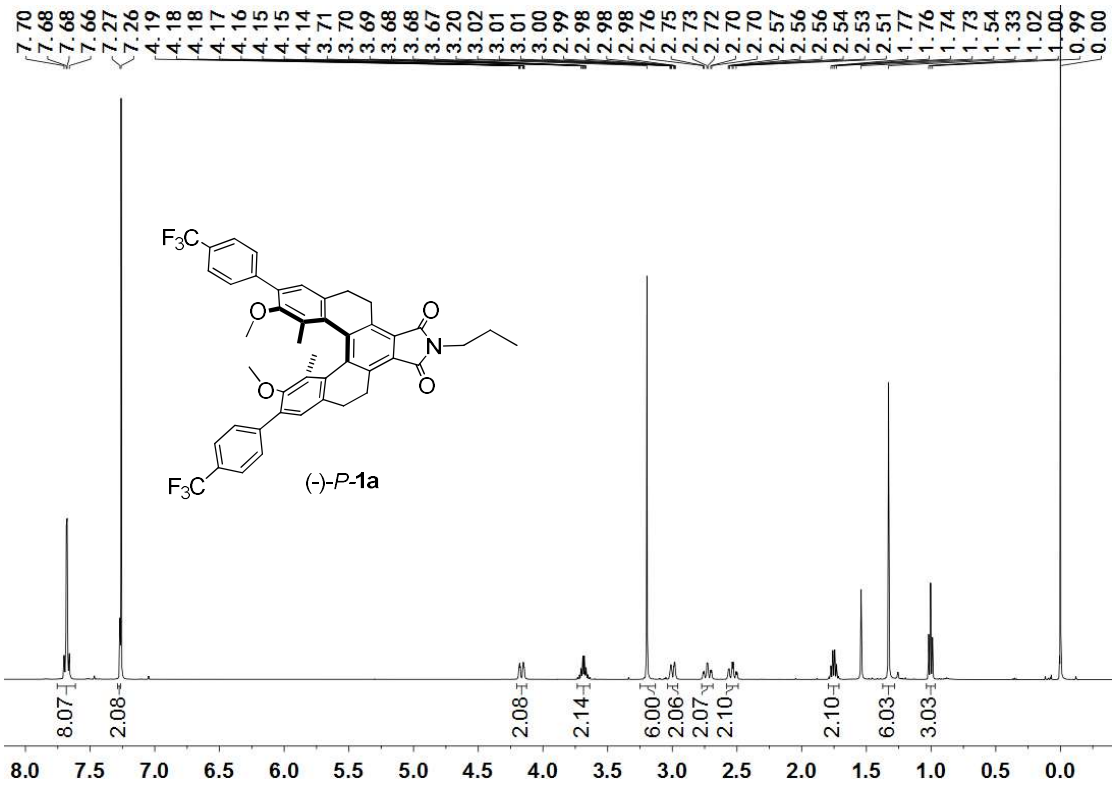

Fig. S26. ^{1}H NMR spectrum (500 MHz, $CDCl_3$) of (–)-*P*-**1a**.

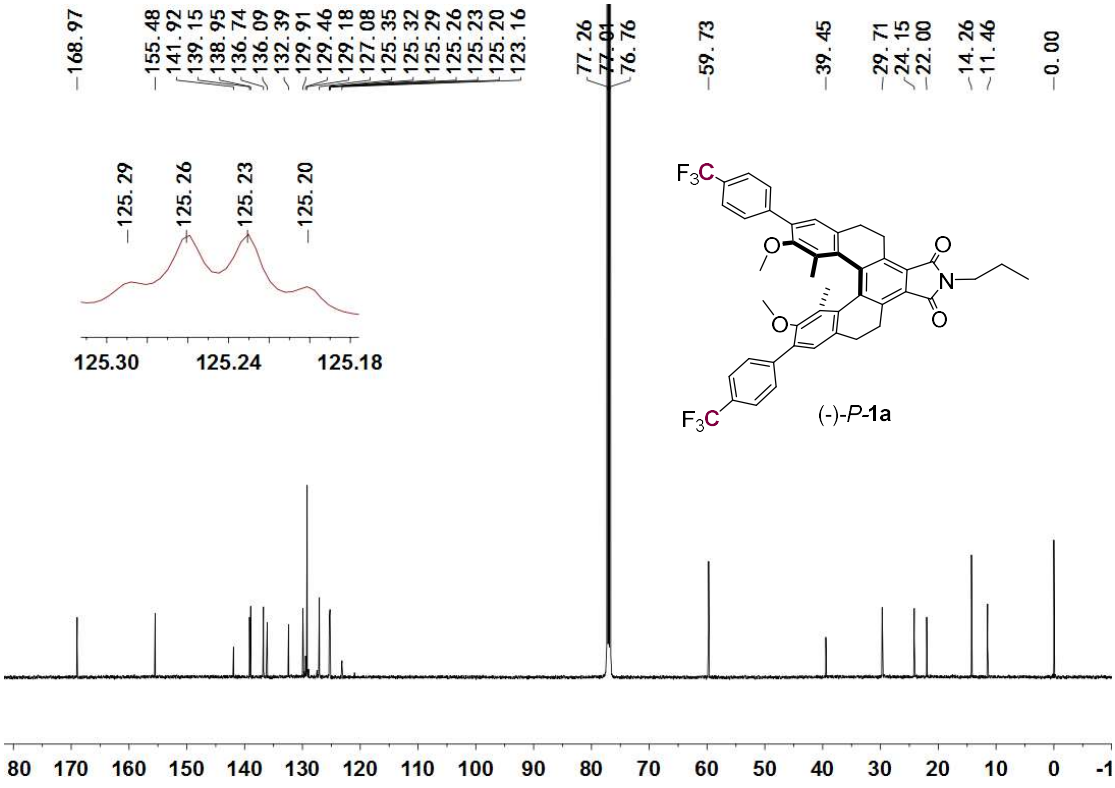

Fig. S27. ^{13}C NMR spectrum (126 MHz, $CDCl_3$) of (–)-*P*-**1a**.

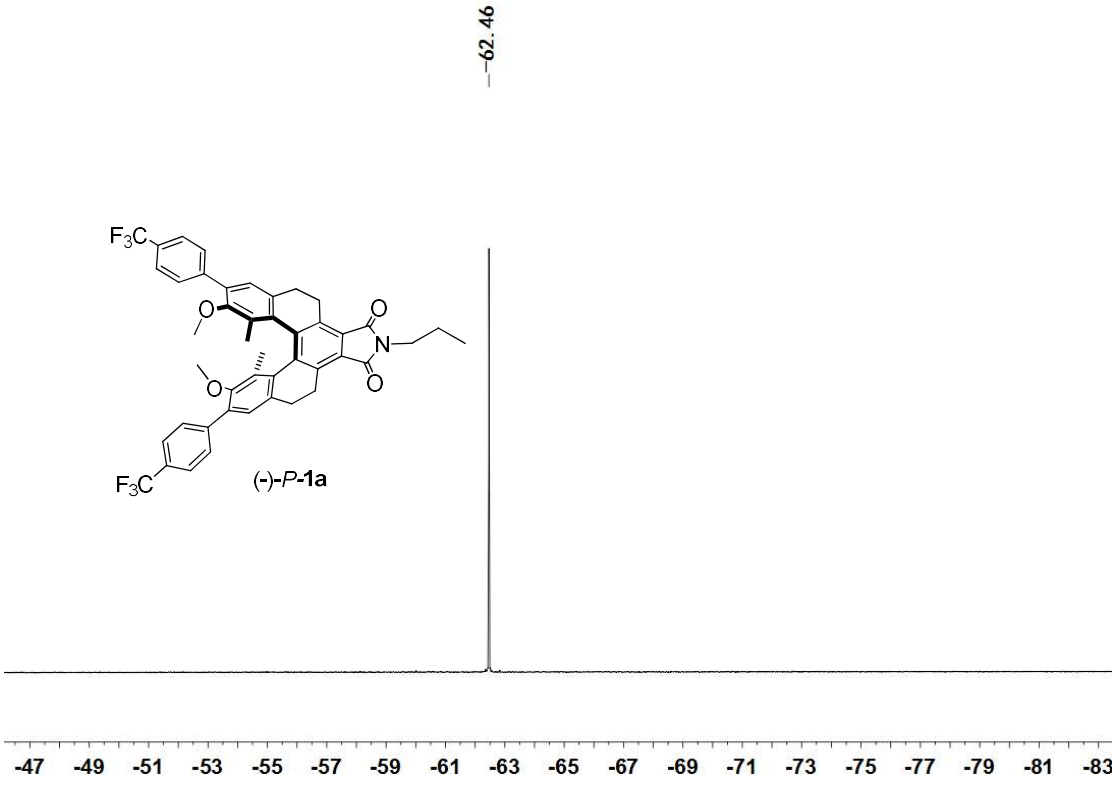

Fig. S28. ^{19}F NMR spectrum (565 MHz, $CDCl_3$) of (–)-*P*-**1a**.

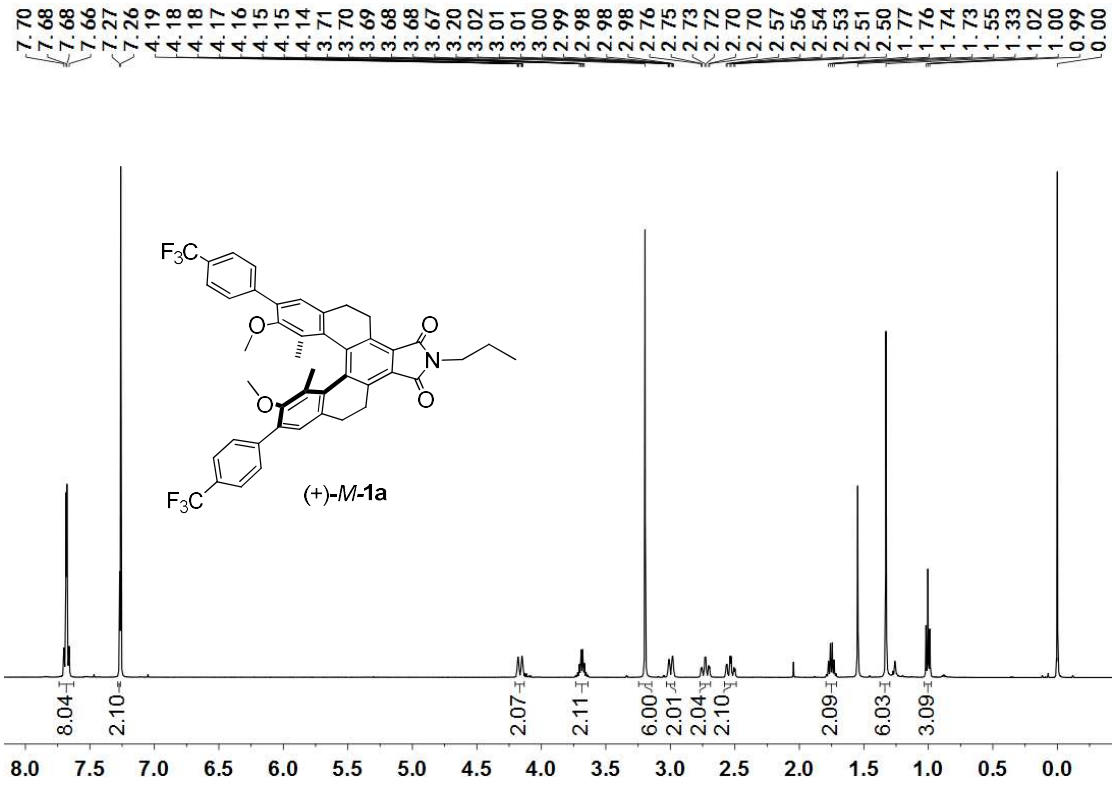

Fig. S29. ^{1}H NMR spectrum (500 MHz, $CDCl_3$) of (+)-*M*-**1a**.

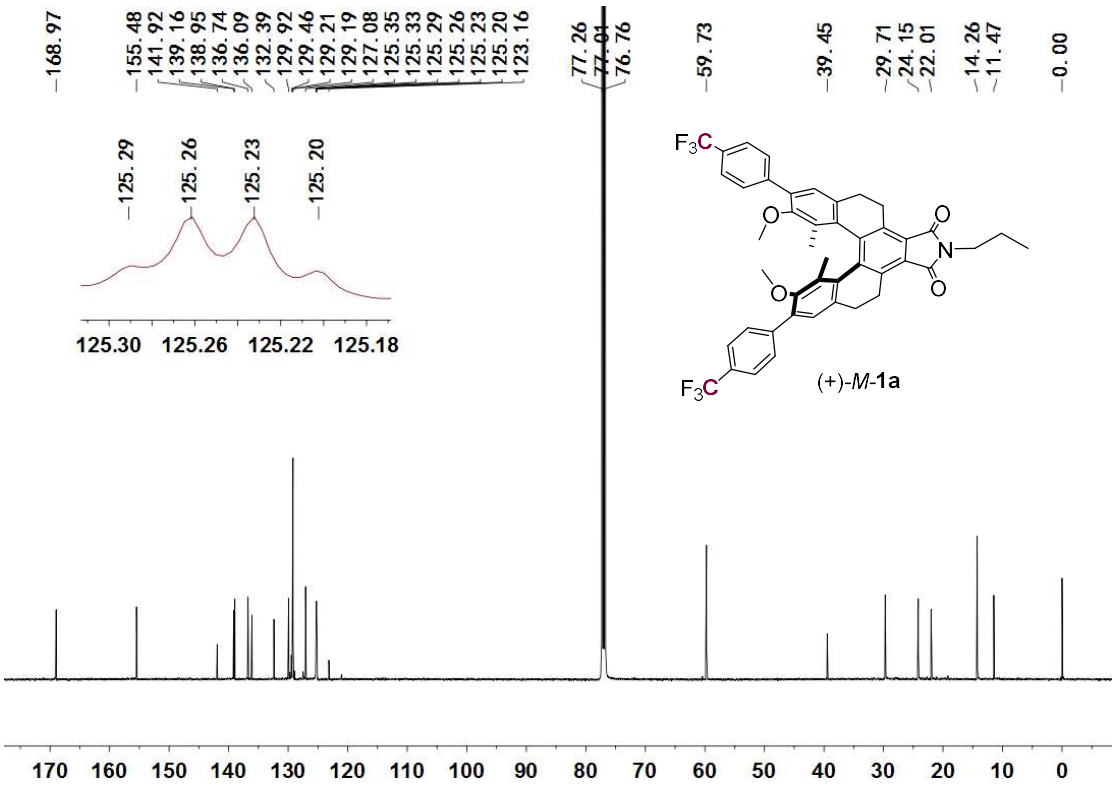

Fig. S30. ^{13}C NMR spectrum (126 MHz, $CDCl_3$) of (+)-*M*-**1a**.

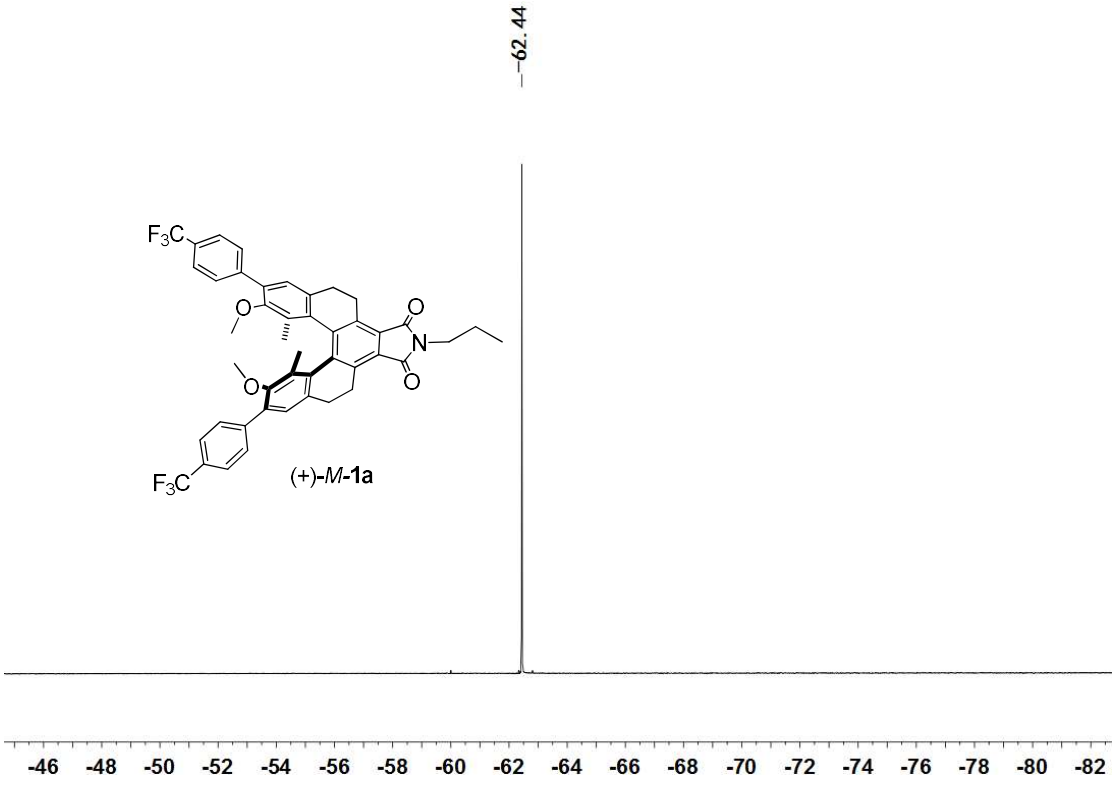

Fig. S31. ^{19}F NMR spectrum (565 MHz, $CDCl_3$) of (+)-*M*-**1a**.

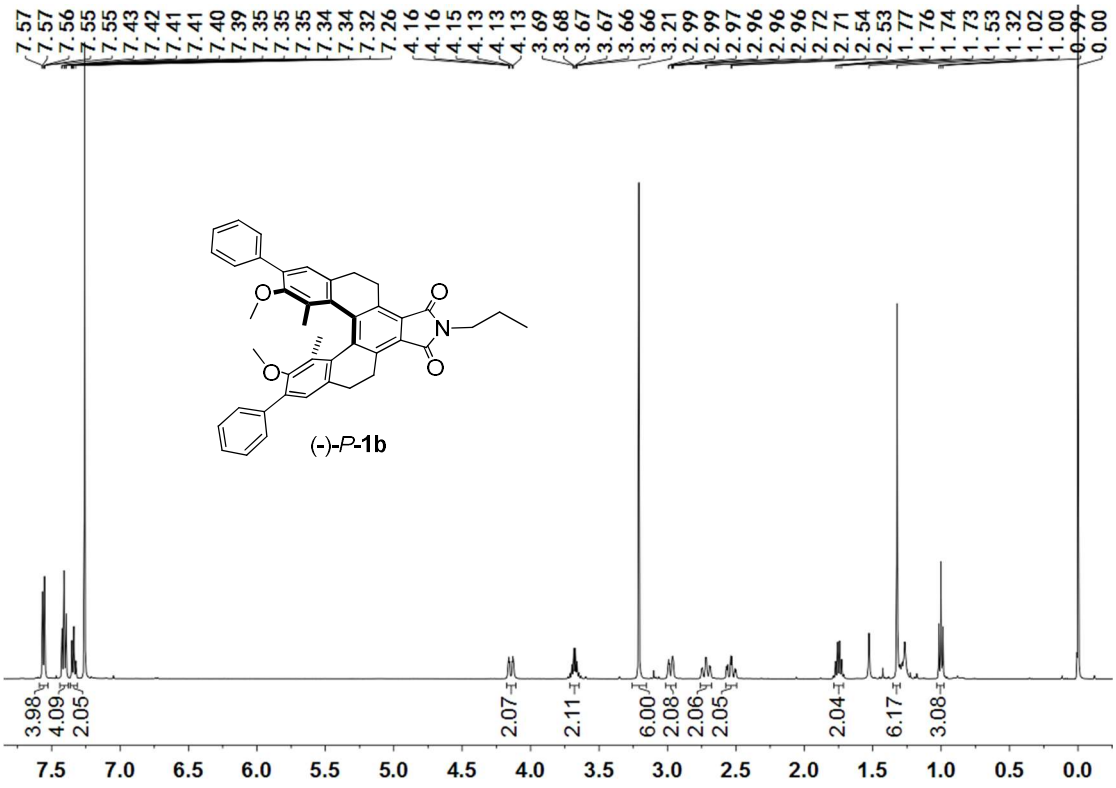

Fig. S32. ^{1}H NMR spectrum (500 MHz, $CDCl_3$) of (–)-*P*-**1b**.

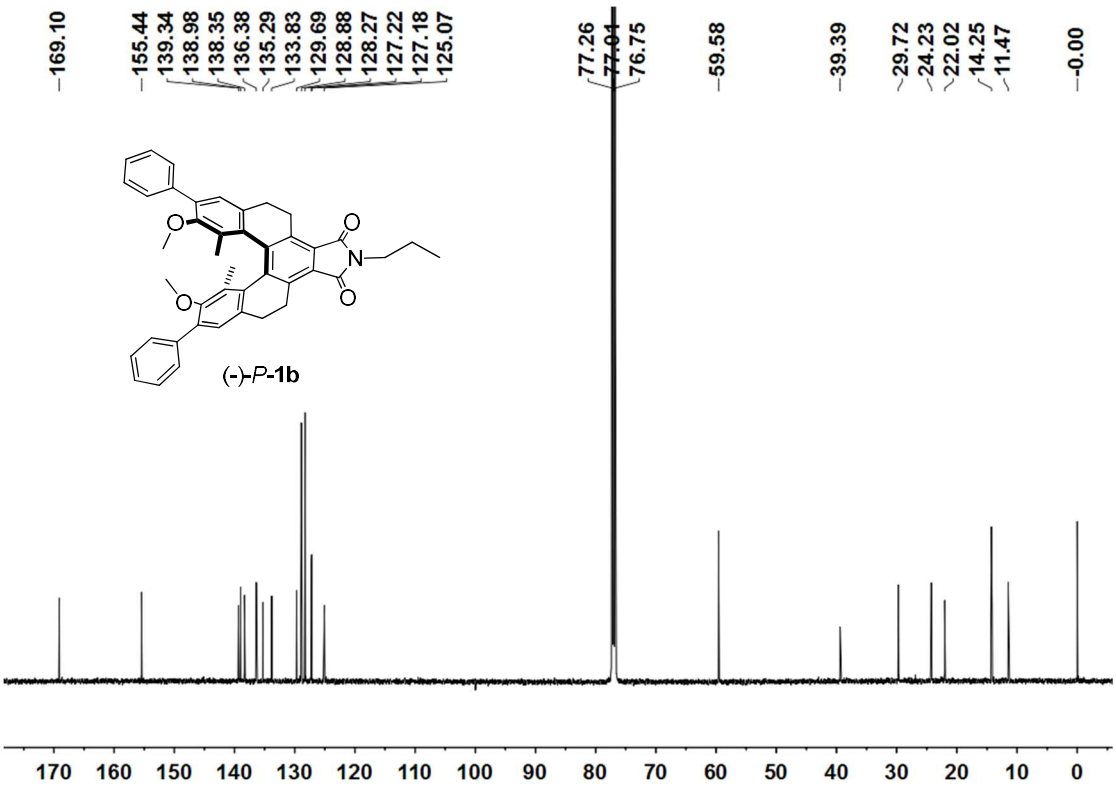

Fig. S33. ^{13}C NMR spectrum (126 MHz, $CDCl_3$) of (–)-*P*-**1b**.

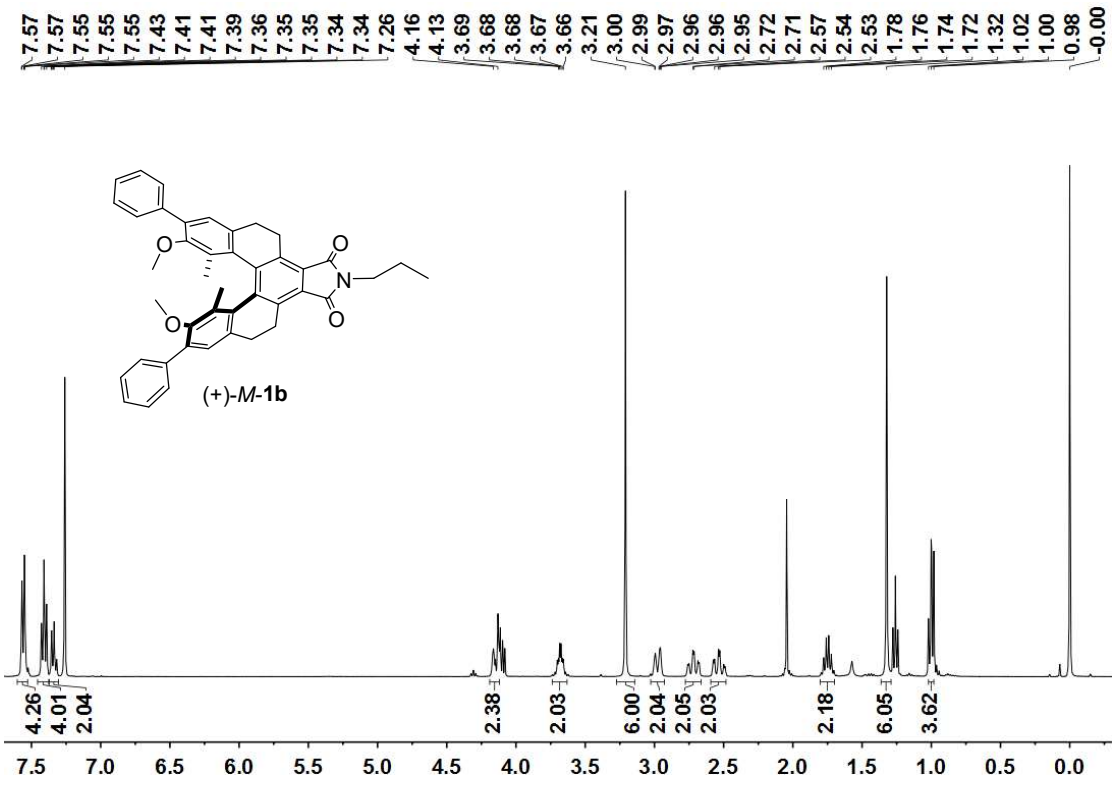

Fig. S34. ^{1}H NMR spectrum (400 MHz, $CDCl_3$) of (+)-*M*-**1b**.

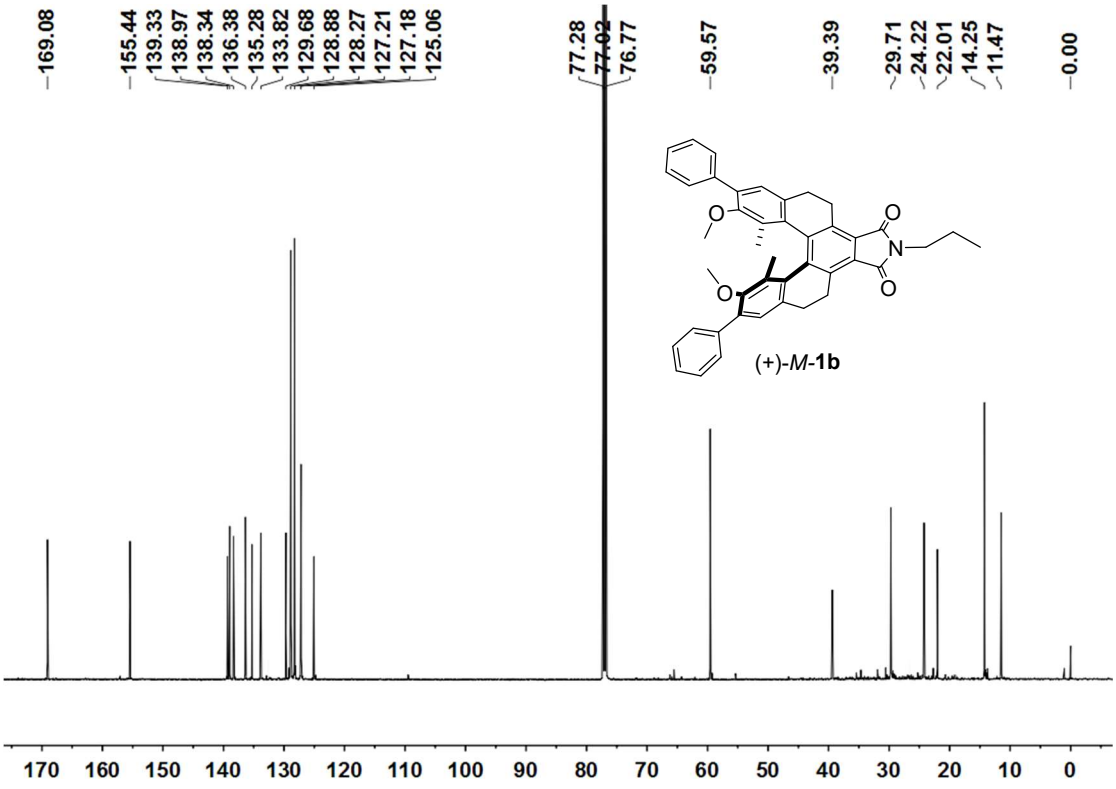

Fig. S35. ^{13}C NMR spectrum (126 MHz, $CDCl_3$) of (+)-*M*-**1b**.

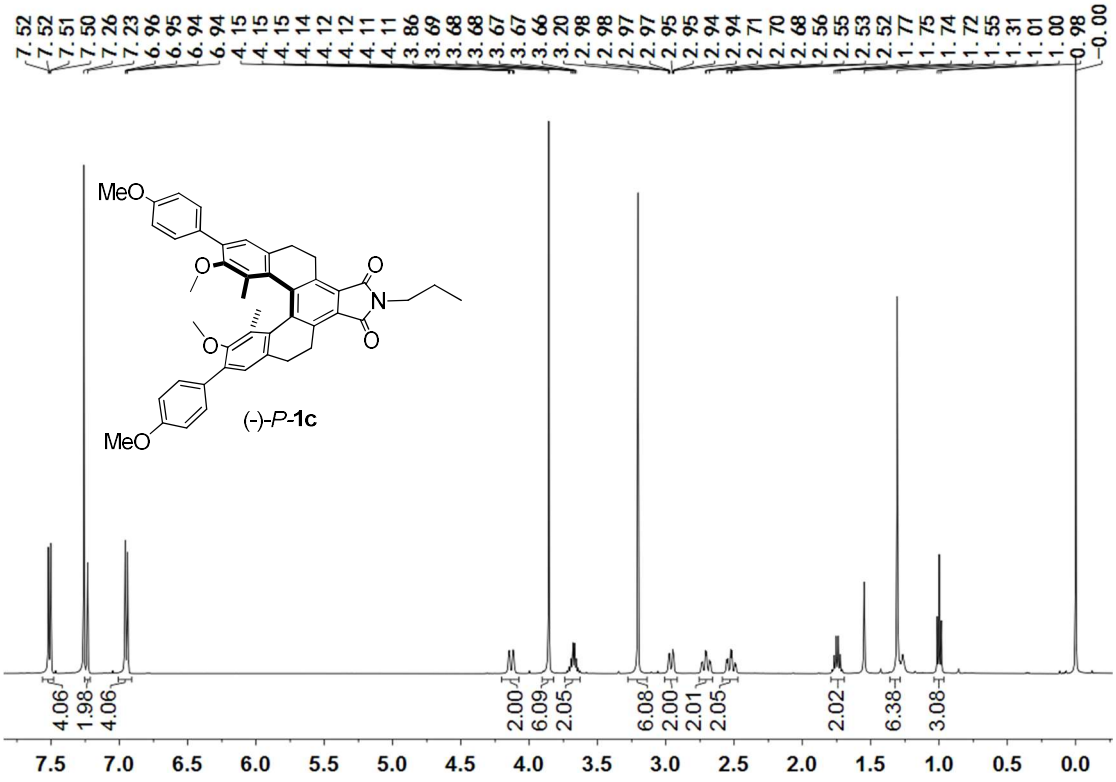

Fig. S36. ^{1}H NMR spectrum (500 MHz, $CDCl_3$) of (–)-*P*-**1c**.

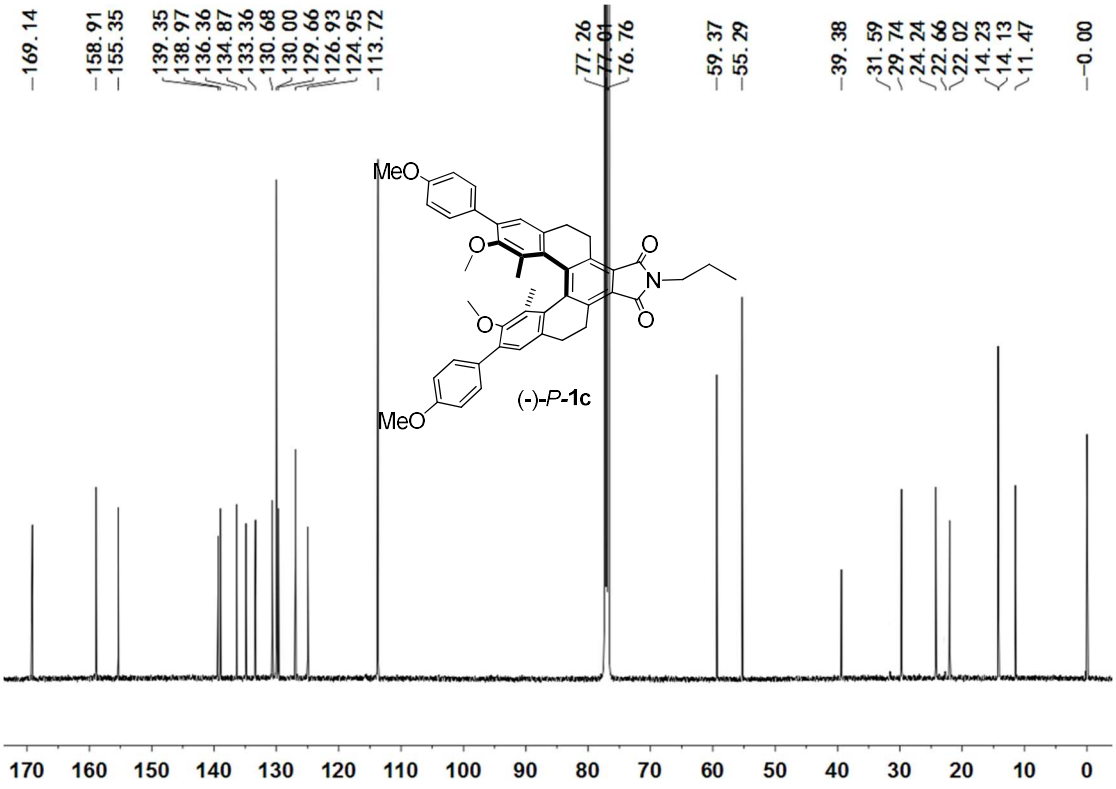

Fig. S37. ^{13}C NMR spectrum (126 MHz, $CDCl_3$) of (–)-*P*-**1c**.

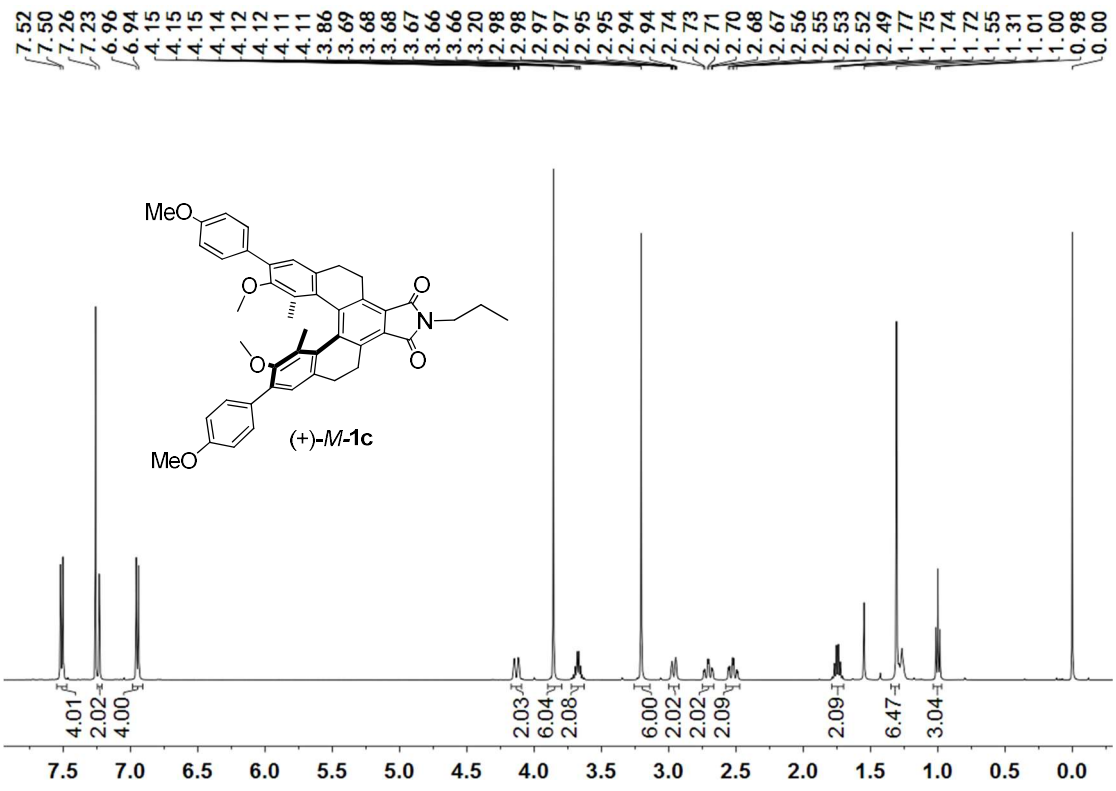

Fig. S38. ^{1}H NMR spectrum (500 MHz, $CDCl_3$) of (+)-*M*-**1c**.

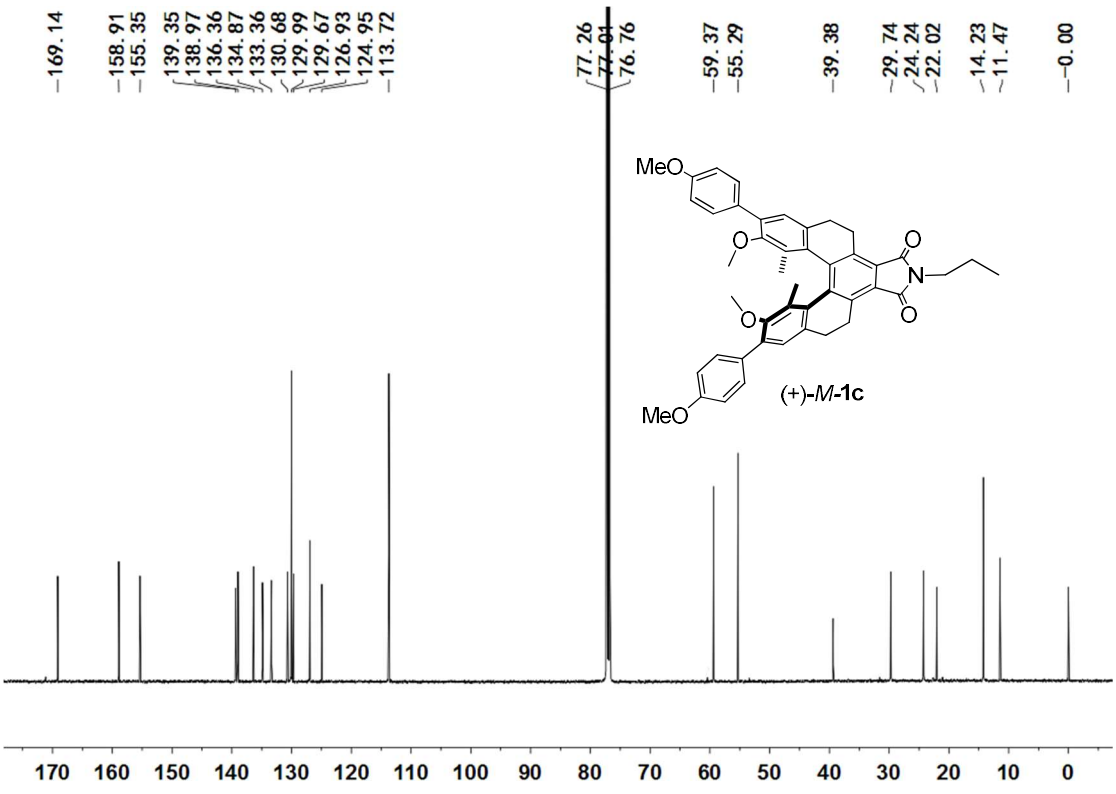

Fig. S39. ^{13}C NMR spectrum (126 MHz, $CDCl_3$) of (+)-*M*-**1c**.

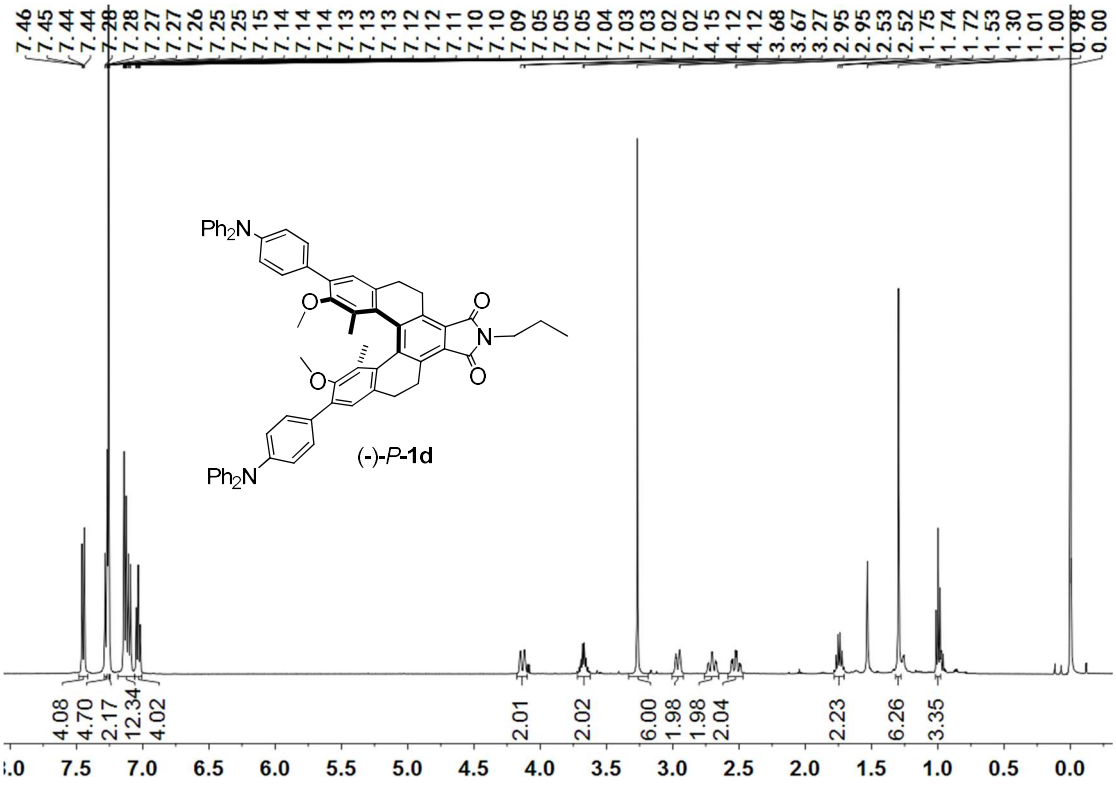

Fig. S40. ^{1}H NMR spectrum (500 MHz, $CDCl_3$) of (–)-*P*-**1d**.

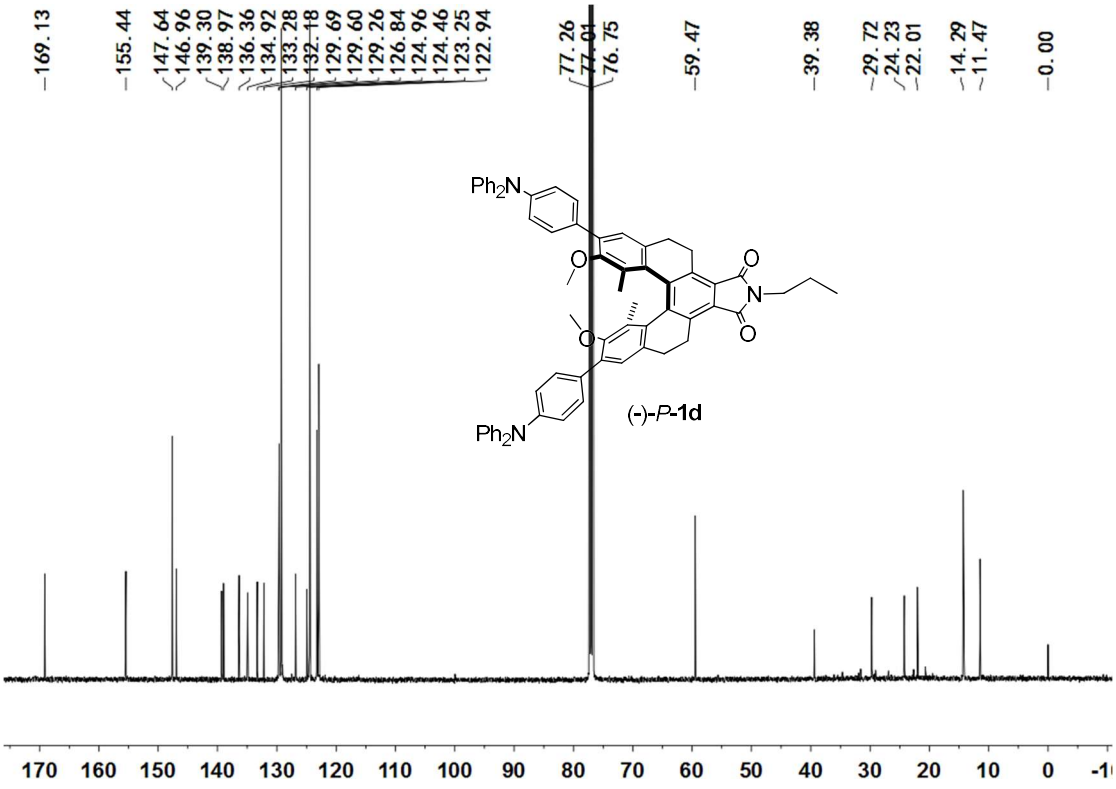

Fig. S41. ^{13}C NMR spectrum (126 MHz, $CDCl_3$) of (–)-*P*-**1d**.

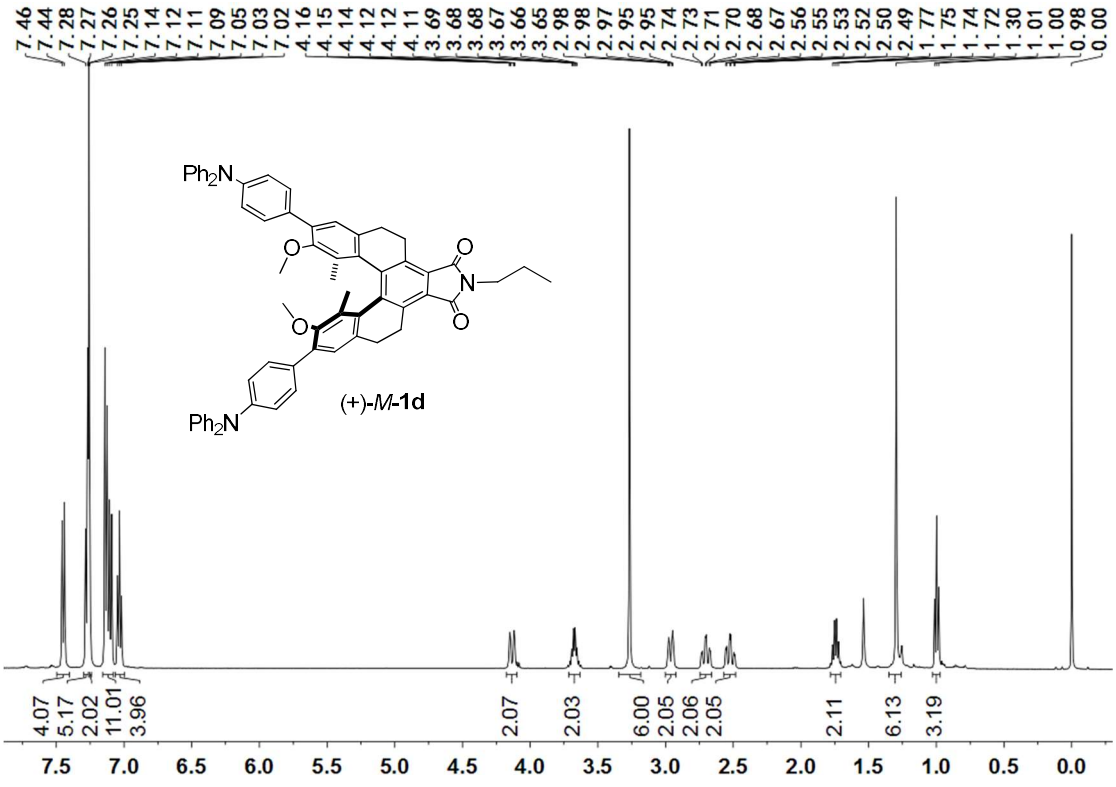

Fig. S42. ^{1}H NMR spectrum (500 MHz, $CDCl_3$) of (+)-*M*-**1d**.

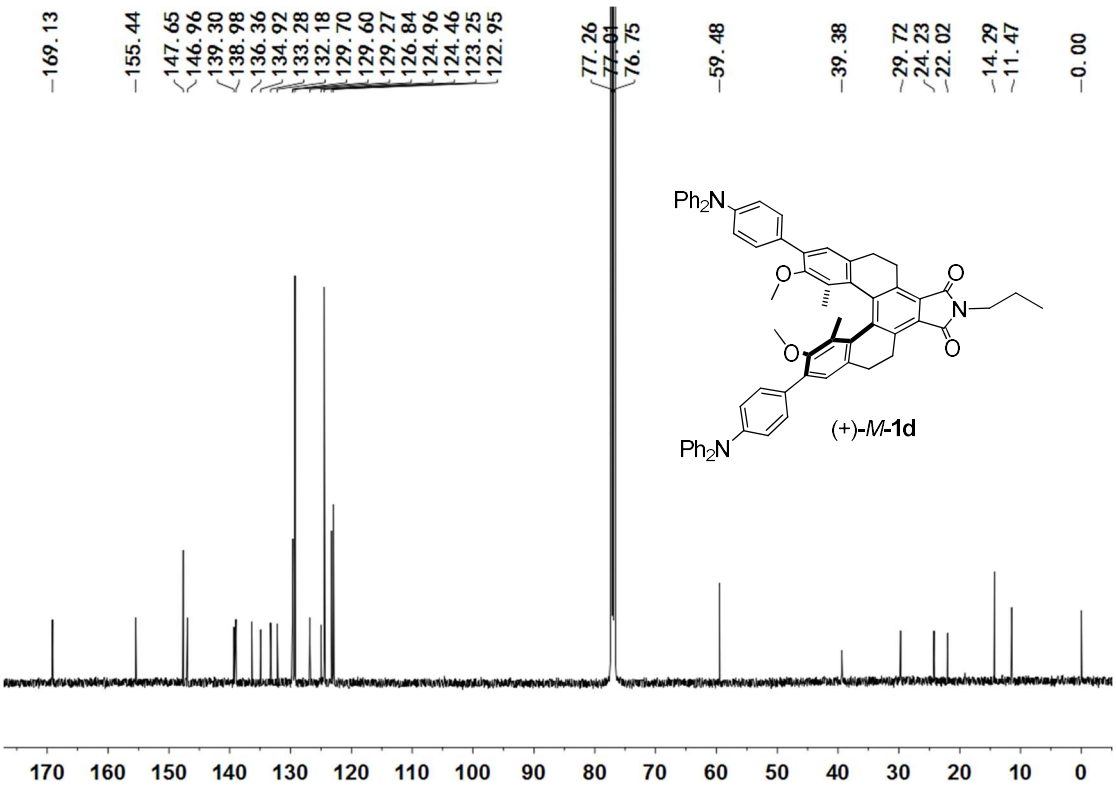

Fig. S43. ^{13}C NMR spectrum (126 MHz, $CDCl_3$) of (+)-*M*-**1d**.

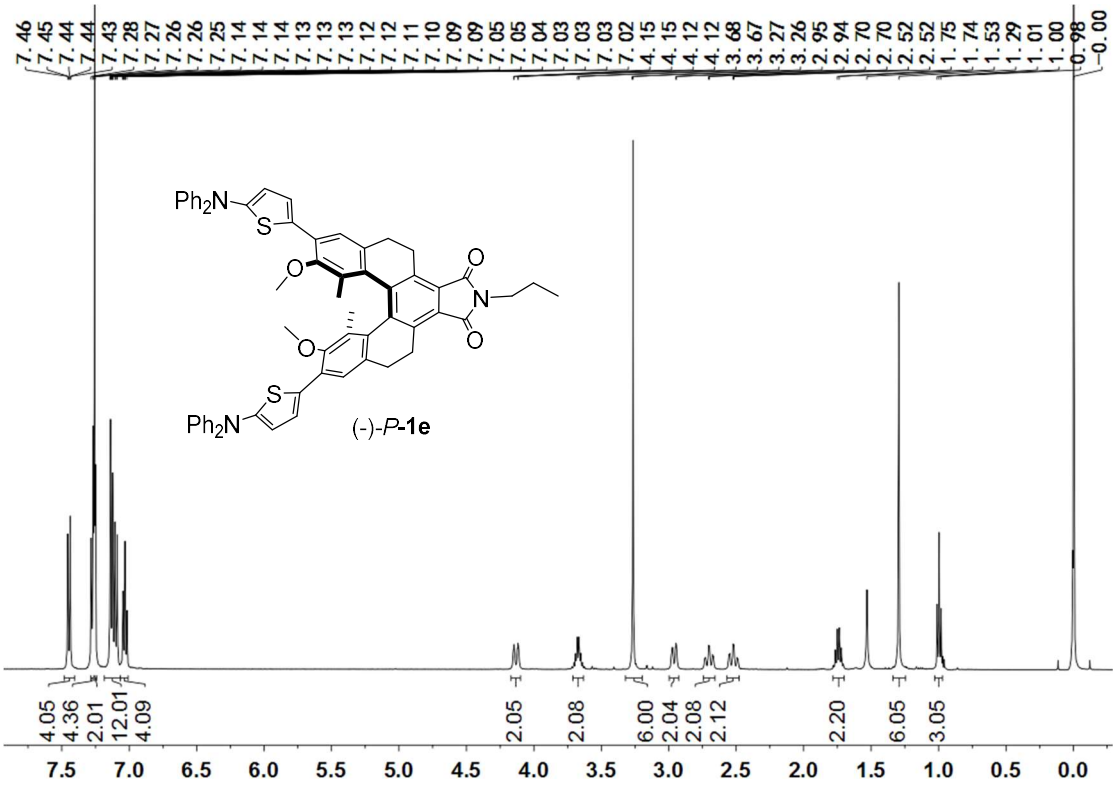

Fig. S44. ^{1}H NMR spectrum (500 MHz, $CDCl_3$) of (–)-*P*-**1e**.

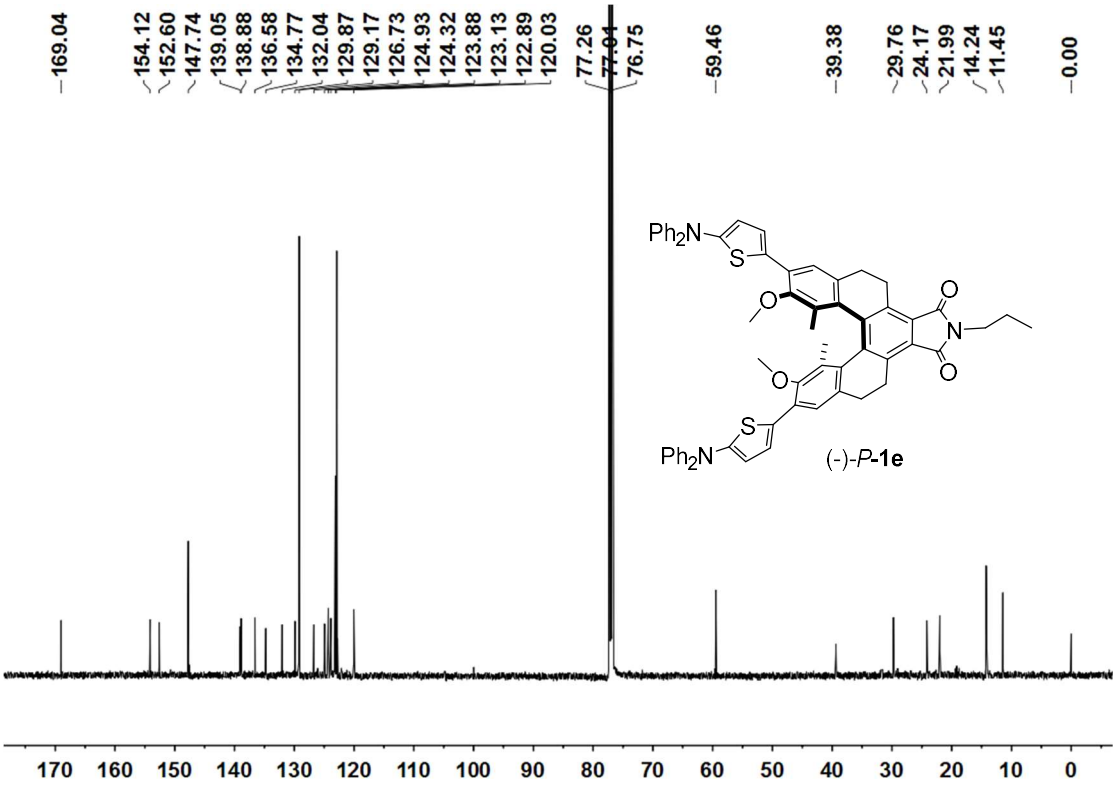

Fig. S45. ^{13}C NMR spectrum (126 MHz, $CDCl_3$) of (–)-*P*-**1e**.

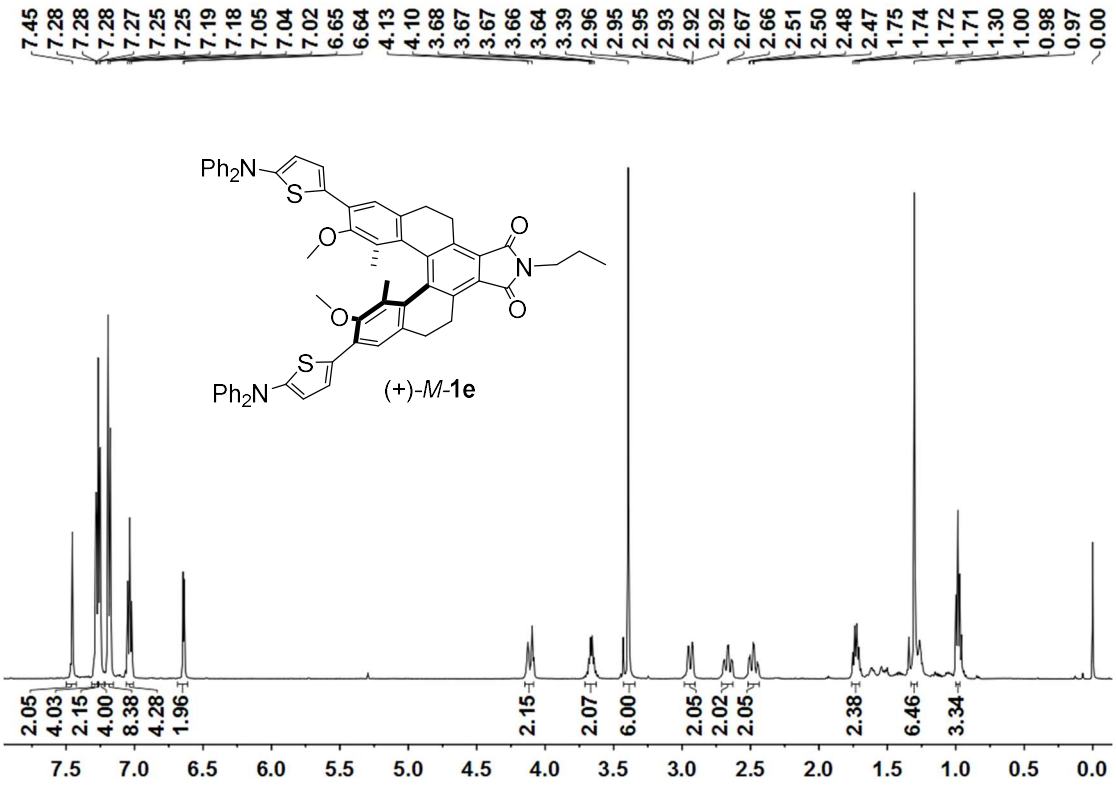

Fig. S46. ^{1}H NMR spectrum (500 MHz, $CDCl_3$) of (+)-*M*-**1e**.

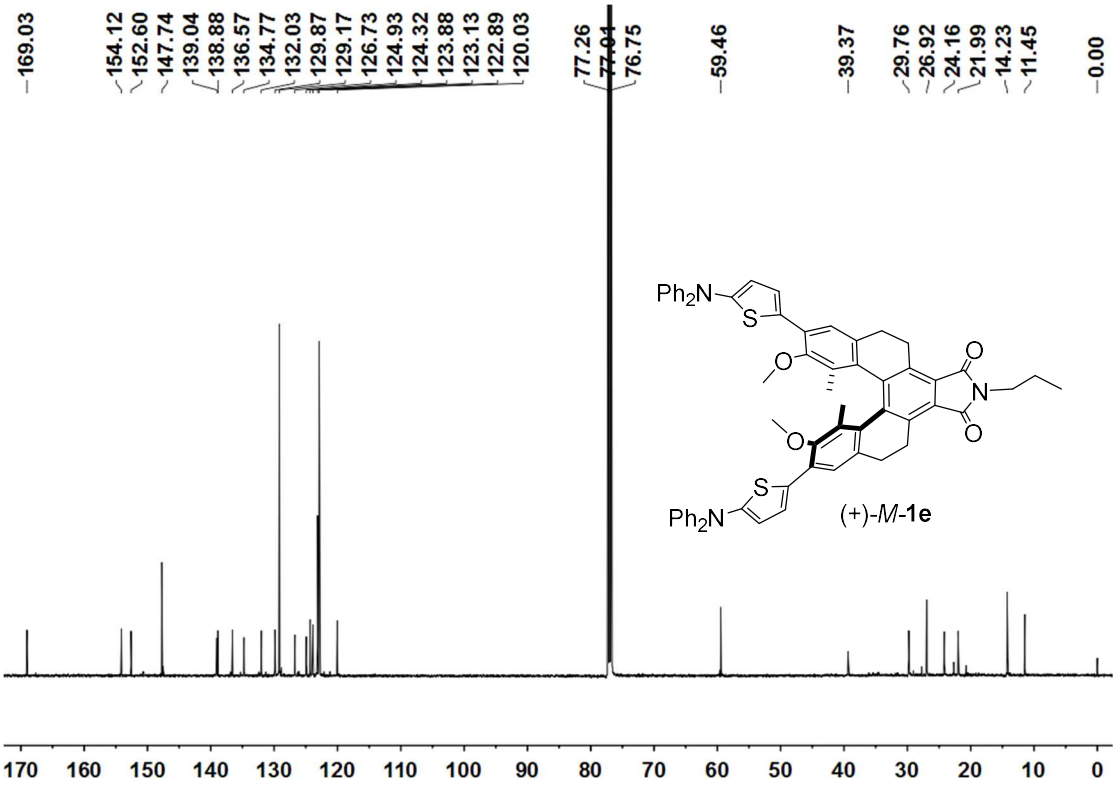

Fig. S47. ^{13}C NMR spectrum (126 MHz, $CDCl_3$) of (+)-*M*-**1e**.